Ligand Dependence of the Indenyl Ring Slippage in $[(\eta^5\text{-Ind})MoL_2(CO)_2]^{0,+}$ Complexes: Experimental and Theoretical Studies

Maria J. Calhorda,[†,‡] Carla A. Gamelas,[†,§] Isabel S. Gonçalves,[†,||] Eberhardt Herdtweck,[⊥] Carlos C. Romão,*[,†] and Luís F. Veiros[#]

Instituto de Tecnologia Química e Biológica, Quinta do Marquês, EAN, Apt 127, 2780 Oeiras, Portugal, Departamento Química e Bioquímica, Faculdade de Ciências, Universidade de Lisboa, 1700 Lisboa, Portugal, Escola Superior de Tecnologia, Instituto Politécnico de Setúbal, 2900 Setúbal, Portugal, Departamento Química, Universidade de Aveiro, Campus de Santiago, 3800 Aveiro, Portugal, Anorganisch-chemisches Institut, Technische Universität München, D-85478 Garching, Federal Republic of Germany, and Centro de Química Estrutural, Instituto Superior Técnico, 1096 Lisboa Codex, Portugal

Received November 14, 1997

The reaction of a series of cationic and neutral complexes $[(\eta^5\text{-Ind})Mo(CO)_2L_2]^{0,+}$ (**1**, L = NCMe; **2**, L = CNMe; **3**, L = $OPPh_3$; **4**, L = $OP(OMe)_3$; **5**, L = PMe_3; **6**, $L_2 = (PhSCH_2)_2$; **7**, $L_2 = (O_2CCF_3)^-$; **8**, $L_2 = (O_2CCH_3)^-$; **9**, $L_2 = (O_2CPh)^-$; **10**, $L_2 = [(NPh)_2CH]^-$; **11**, $L_2 = [(N\text{-}p\text{-tolyl})_2CH]^-$; **12**, $L_2 = (S_2CNEt_2)^-$; **13**, $L_2 = (S_2P(OEt)_2)^-$; **14**, $L_2 = acac^-$; **15**, L_2 = MeC(O)CHC(NPh)CMe) with acetonitrile produces the ring-slipped adducts $[(\eta^3\text{-Ind})MoL_2(NCMe)(CO)_2]^{0,+}$ only in the cases where L = NCMe, $OPPh_3$, $OP(OMe)_3$ or $L_2 = (O_2CCF_3)^-$, $acac^-$. The adducts are labile and have been characterized by means of the distinctive chemical shift of the central pseudo-allylic proton of the η^3-indenyl ligand. In the other cases no ring slippage is observed. In NCMe solvent **6** undergoes substitution to give **1**, but the macrocycle trithiacyclononane (ttcn) reacts with **1** to give $[(\eta^3\text{-Ind})Mo(CO)_2(\kappa^3\text{-ttcn})]^+$ as the BF_4^- salt. PMe_3 reacts with **1** to give substitution products in a stepwise fashion. $[(\eta^5\text{-Ind})Mo(NCMe)(PMe_3)(CO)_2]BF_4$ is formed instantaneously at −70 °C, but **5** forms slowly at room temperature without any detectable ring-slipped intermediate. The crystal structure of the isonitrile cation **2** is presented. **2** adds neither NCMe nor CNMe but undergoes CO substitution with excess CNMe. Extended Hückel and density function calculations predict the most stable conformation of $[(\eta^5\text{-Ind})MoL_2(CO)_2]^+$ (L = NCR, CNR) to be the one with the ring trans to the carbonyls, while for the $[(\eta^3\text{-Ind})MoL_2(NCR)(CO)_2]^+$ complexes the ring lies over the carbonyls. According to the dft calculations, acetonitrile addition induces $\eta^5 \rightarrow \eta^3$ slipping of the ring in the NCR derivatives but not in the CNR analogues, because the reaction is enthalpically driven in the former and not in the latter. The dft calculations of part of the reaction path indicate that the indenyl ring starts to slip when the incoming ligand is still far from the metal (∼400 pm), thus supporting earlier kinetically based proposals.

Introduction

The haptotropic rearrangement of coordinated polyenyl ligands is a well-established process by which the metal adjusts its total electron count (usually 18e) upon addition or removal of other ligands (or electrons) to or from the coordination sphere. Where cyclic polyenyl ligands are concerned, this process is casually termed "ring slippage" and has been reviewed for the cyclopentadienyl (Cp) and indenyl (Ind) ligands.[1] In the latter case, ring slippage is considered as particularly important, since it is associated with distinct and sometimes rather large rate accelerations in substitution reactions of $IndML_n$ complexes in comparison to the reactions of their Cp analogues. This rate acceleration, or indenyl effect as it was called by Basolo,[2] certainly plays an important role in some catalytic reactions performed by indenyl complexes.[3]

Kinetic studies revealed that the indenyl effect is felt in both dissociative (S_N1) and associative (S_N2) reaction pathways. As discussed by Basolo, the latter are more common and involve a larger rate enhancement.[4] The widely accepted explanation of this effect was first

† Instituto de Tecnologia Química e Biológica.
‡ Universidade de Lisboa.
§ Instituto Politécnico de Setúbal.
|| Universidade de Aveiro.
⊥ Technische Universität München.
Instituto Superior Técnico.

(1) O'Connor, J. M.; Casey, C. P. *Chem. Rev.* **1987**, *87*, 307.

(2) Rerek, M. E.; Ji, L.-N.; Basolo, F. *J. Chem. Soc., Chem. Commun.* **1983**, 1208.

(3) (a) Marder, T. B.; Roe, D. C.; Milstein, D. *Organometallics* **1988**, *7*, 1451. (b) Borrini, A.; Diversi, P.; Ingrosso, G.; Lucherini, A.; Serra, G., *J. Mol. Catal.* **1985**, *30*, 181. (c) Bönnemann, H. *Angew. Chem., Int. Ed. Engl.* **1985**, *24*, 248. (d) Foo, T.; Bergman, R. G. *Organometallics* **1992**, *11*, 1801. (e) Schmid, M. A.; Alt, H. G.; Milius, W. *J. Organomet. Chem.* **1996**, *514*, 45. (f) Llinas, G. H.; Day, R. O.; Rausch, M. D.; Chien, J. C. W. *Organometallics* **1993**, *12*, 1283.

(4) Ji, L.-N.; Rerek, M. E.; Basolo, F. *Organometallics* **1984**, *3*, 740.

S0276-7333(97)01005-4 CCC: $15.00
Publication on Web 05/13/1998

Chart 1

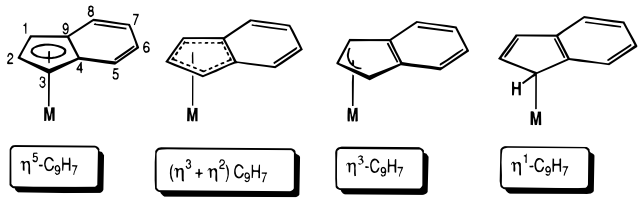

proposed by Hart-Davis and Mawby: attack of an incoming nucleophile in an associative pathway is made easier by a low-energy $\eta^5 \rightarrow \eta^3$ ring slippage of the indenyl ligand which avoids a transition state with more than 18 electrons at the metal.[5] However, the kinetic data are also consistent with a preequilibrium between η^5 and η^3 forms of the starting complex, where the latter species reacts with the entering nucleophile in a rate-determining step.[4] In any case, the low energy barrier for the slippage is provided by the resonance stabilization of the benzene ring which is regained in the η^3 coordination mode.

In keeping with these easy ring slippage rearrangements crystallographic studies have revealed a variety of coordination modes of the indenyl ligand. Chart 1 summarizes the most important situations when only the five-membered ring coordination is concerned.

Pure η^5 coordination, i.e, with all five carbons of the ring equidistant from the metal and a planar indenyl system, is rare but has been observed, inter alia, for Ind_2Fe and closely related metallocene analogues[6a] and has been studied from a molecular orbital point of view.[6b] Pure η^3 coordination is also very well characterized in both transition-metal[7] and main-group indenyl complexes.[8] In this situation the C1, C2, and C3 atoms are equidistant and bound to the metal. The ring junction atoms C4 and C9 lie outside the bond distance range, and the indenyl ring loses planarity. A number of geometrical parameters and NMR chemical shifts have been used to describe these distortions. In the present paper we use the set of parameters proposed by Faller, Crabtree, and Habib,[9] which are closely related to the ones used in the works of Marder and Taylor[10] and Baker,[11a] as discussed in ref 6. The initial observation of a downfield shift of the ^{13}C chemical shifts of the C4 and C9 atoms in Ind_2Ni[11b] was later confirmed by the existence of a very sensitive correlation between the indenyl distortion and the value of those chemical shifts.[11a]

η^1 coordination has also been well characterized and is associated with fluxional behavior between the C1 and C3 bonding positions.[1,12] Coordination of the indenyl anion via the six-membered ring has been observed in $[(\eta^5\text{-Ind})(\eta^6\text{-Ind})Re]K$[13] as well as the simultaneous coordination of both rings to different transition metals, as in $Cr(CO)_3(\mu\text{-}\eta\text{:}\eta\text{-indenyl})RhL_2$ species.[14]

The situation termed as $\eta^3 + \eta^2$ coordination in Chart 1 is intermediate between η^5 and η^3 coordination and seems to be the most common one in indenyl chemistry. Although almost undistorted η^5 coordination has been observed in the 18e metallocenes such as Ind_2M (M = Fe, Ru) and $[Ind_2Co]^+$,[6a] most 18-electron compounds with formal η^5 coordination show this kind of slip-fold distortion as first noted and summarized by Faller.[9] More recent examples comprise the systematic study that revealed this type of distortion in all members of a variety of d^8-$[IndRhL_2]$ complexes[10,11] as well as in the formally 16e ethylene-selective polymerization catalyst $Cp^*(Ind)ZrCl_2$.[3e] A comparative analysis of the structures of many $IndML_nL'_m$ complexes led to a rule of thumb which states that the benzene ring of the indenyl points away from the metal in the direction opposite to the most strongly trans director ancillary L (or L′) ligand.[9] This quite general rule seems to imply that electronic factors are the ones responsible for the slip-fold distortion. In the comparative study carried out with metallocenes,[6a] it could be clearly shown that addition of electrons to the metal results in ring slippage and indenyl distortion to avoid 19 and 20 formal electron counts as in Ind_2Co and Ind_2Ni, respectively. Recently, we have noted that the 2e oxidation of $(\eta^3\text{-Ind})CpM(CO)_2$ leads to $[(\eta^5\text{-Ind})CpMo(CO)_2]^{2+}$, and preliminary results show that this is a chemically and electrochemically reversible process.[7e,f,15] On the other hand, less information is available on the influence of one incoming ligand (2e donor) upon the ring slippage process. Furthermore, not much is known about the influence of steric factors on the ring-slippage and slip-fold processes. A systematic variation of the degree of substitution of the indenyl ring in $(\eta\text{-}C_6H_{7-x}R_x)Rh(CO)_2$ complexes led to essentially unchanged structural characteristics of the indenyl distortion in the ground state.[16] However, steric factors do play a role as the kinetic data have already established, for associative substitution reactions of several $IndM(CO)_n$ (M = Mn, $n = 3$;[4] M= Rh, $n = 2$[16]) complexes were found to be dependent on the basicity, the size, and the chemical nature of the entering nucleophile.

(5) Hart-Davis, A. J.; Mawby, R. J. *J. Chem. Soc. A* **1969**, 2403.

(6) (a) Westcott, S. A.; Kakkar, A. K.; Stringer, G.; Taylor, N. J.; Marder, T. B. *J. Organomet. Chem.* **1990**, *394*, 777. (b) Crossley, N. S.; Green, J. C.; Nagy, A.; Stringer, G. *J. Chem. Soc., Dalton Trans.* **1989**, 2139.

(7) (a) Merola, J. S.; Kacmarcik, R. T.; Van Engen, D. *J. Am. Chem. Soc.* **1986**, *108*, 329. (b) Forschner, T. C.; Cutler, A. R.; Kullnig, R. K. *Organometallics* **1987**, *6*, 889. (c) Kowalewski, R. M.; Rheingold, A. L.; Trogler, W. C.; Basolo, F. *J. Am. Chem. Soc.* **1986**, 108, 2460. (d) Poli, R.; Mattamana, S. P.; Falvello, L. R. *Gazz. Chim. Ital.* **1992**, *122*, 315. (e) Ascenso, J. R.; Azevedo, C. G.; Gonçalves, I. S.; Herdtweck, E.; Moreno, D. S.; Romão, C. C.; Zühlke, J. *Organometallics* **1994**, *13*, 429. (f) Ascenso, J. R.; Azevedo, C. G.; Gonçalves, I. S.; Herdtweck, E.; Moreno, D. S.; Pessanha, M.; Romão, C. C. *Organometallics* **1995**, *14*, 3901. (g) Gonçalves, I. S.; Romão, C. C. *J. Organomet. Chem.* **1995**, *486*, 155.

(8) Viebrock, H.; Abeln, D.; Weiss, E. *Z. Naturforsch.* **1994**, *49B*, 89.

(9) Faller, J. W.; Crabtree, R. H.; Habib, A. *Organometallics* **1985**, *4*, 929.

(10) (a) Marder, T. B.; Calabrese, J. C.; Roe, D. C.; Tulip, T. H. *Organometallics* **1987**, *6*, 2012. (b) Kakkar, A. K.; Jones, S. F.; Taylor, N. J.; Collins, S.; Marder, T. B. *J. Chem. Soc., Chem. Commun.* **1989**, 1454. (c) Kakkar, A. K.; Taylor, N. J.; Calabrese, J. C.; Nugent, W. A.; Roe, D. C.; Connaway, E. A.; Marder, T. B. *J. Chem. Soc., Chem. Commun.* **1989**, 990. (d) Carl, R. T.; Hughes, R. P.; Rheingold, A. L.; Marder, T. B.; Taylor, N. J. *Organometallics* **1988**, *7*, 1613.

(11) (a) Baker, R. T.; Tulip, T. H. *Organometallics* **1986**, *5*, 839. (b) Köhler, F. H. *Chem. Ber.* **1974**, *107*, 570.

(12) Herrmann, W. A.; Kühn, F. E.; Romão, C. C. *J. Organomet. Chem.* **1995**, *489*, C56 and references therein.

(13) Green, M. L. H.; Lowe, N. D.; O'Hare, D. *J. Organomet. Chem.* **1988**, *355*, 315.

(14) (a) Ceccon, A.; Gambaro, A.; Santi, S.; Valle, G.; Venzo, A. *J. Chem. Soc., Chem. Commun.* **1989**, 51. (b) Ceccon, A.; Elsevier: C. J.; Ernsting, J. M.; Gambaro, A.; Santo, S.; Venzo, A. *Inorg. Chim. Acta* **1993**, *204*, 15.

(15) Calhorda, M. J.; Gamelas, C. A.; Gonçalves, I. S.; Herdtweck, E.; Lopes, J. P.; Romão, C. C.; Veiros, L. Paper presented at the XIIth FECHEM, Prague, Czech Republic, 1997.

(16) Kakkar, A. K.; Taylor, N. J.; Marder, T. B.; Shen, J. K.; Hallinan, N.; Basolo, F. *Inorg. Chim. Acta* **1992**, *198−200*, 219.

In the case of $IndMn(CO)_3$, PR_3 ligands, including the very bulky PCy_3, replace CO but 4-*tert*-butylpyridine is unreactive under the same conditions. Similarly, the addition of $P(^nBu)_3$ to $(\eta^5\text{-Ind})Re(CO)_3$, to give $(\eta^1\text{-Ind})Re(CO)_3\{(P(^nBu)_3\}_2$ is much faster than the corresponding addition of 2,2′-bipyridyl.[17] Regardless of all efforts, no intermediate $(\eta^3\text{-Ind})Re(CO)_3(P(^nBu)_3)$ species could be detected. As a matter of fact, even despite the low activation barrier to associative ligand substitution in $IndML_n$ complexes, provided by the ring slippage process via some kind of transition state or intermediate bearing a η^3-indenyl ligand and the observed thermodynamic and kinetic stability of many such complexes, it is surprising that so few examples have been identified where ligand addition to a $(\eta^5\text{-Ind})ML_n$ species results in isolable or spectroscopically identifiable $[(\eta^3\text{-Ind})ML_nL']$ derivatives. The first characterized examples all involve very electron-rich species, namely, $(\eta^3\text{-Ind})Ir(PMe_2Ph)_3$ (from $(\eta^5\text{-Ind})Ir(C_2H_4)_2$),[7a] $[(\eta^3\text{-Ind})Fe(CO)_3]^-$ (from $(\eta^5\text{-Ind})Fe(CO)_2]^-$,[7b] and $(\eta^5\text{-Ind})(\eta^3\text{-Ind})V(CO)_2$ (from Ind_2V).[7c] More recently we described a number of octahedral complexes of general formula $[(\eta^3\text{-Ind})ML_2L'(CO)_2]BF_4$ which are easily formed by addition of L′ to the parent cations $[(\eta^5\text{-Ind})ML_2(CO)_2]BF_4$ (M = Mo, W) (eq 1).[18] Interestingly enough, addition takes place readily with L = L′ = NCMe but not with L = L′ = PMe_3, thereby showing an unexpected dependence of the reactivity on the nature of L or L′.

$$[(\eta^5\text{-Ind})ML_2(CO)_2]^+ + L' \rightarrow [(\eta^3\text{-Ind})ML_2L'(CO)_2]^+ \quad (1)$$

Also somewhat unexpected is the fact that the cationic complex $[(\eta^3\text{-Ind})W(NCMe)_3(CO)_2]BF_4$ bears a rather bent indenyl ligand with slip-fold angles of 24.1 and 27.4° for two independent molecules,[18] a value close to the one found for the very electron rich $(\eta^3\text{-Ind})Ir(PMe_2Ph)_3$ (28°).[7a]

In the present paper we extend these studies to other 18e neutral and cationic four-legged piano stool complexes, $[(\eta^5\text{-Ind})ML_2(CO)_2]^{0,+}$, and complete them with EHMO and DFT calculations aimed at understanding the electronic and stereochemical features that govern the $\eta^5 \rightarrow \eta^3$ haptotropic shift in this system as a function of the nature of the ancillary ligands involved in the process. In an attempt to separate electronic from steric effects, the calculations are mainly performed on the isomeric complexes $[(\eta^5\text{-Ind})Mo(NCMe)_2(CO)_2]^+$ and $[(\eta^5\text{-Ind})Mo(CNMe)_2(CO)_2]^+$, which show strikingly different behaviors in addition reactions.

Chemical Studies

Synthesis and Characterization of the $[(\eta^5\text{-Ind})ML_2(CO)_2]^{0,+}$ Complexes. The cationic complexes used in this work are presented in Chart 2, and their synthesis follows the general method summarized in eq 2.[7e−g,19]

Under the same reaction conditions, use of negatively charged bidentate ligands (L_2^-), instead of neutral monodentate L or bidentate L_2, produces the neutral complexes presented in Chart 3.

Chart 2. Cationic Complexes of Type $[(\eta^5\text{-Ind})MoL_2(CO)_2]BF_4$ Prepared as in Eq 2

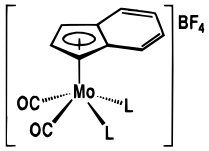

L	Nr.	Ref.
NCMe	1	[6]
CNMe	2	This work
$OPPh_3$	3	This work
$OP(OMe)_3$	4	This work
PMe_3	5	[6]
$(PhSCH_2)_2$	6	This work

Chart 3. Neutral Complexes of Type $[(\eta^5\text{-Ind})Mo(L{-}L)(CO)_2]$ Prepared as in Eq 2

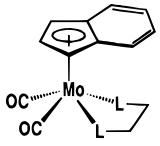

L L	Nr.
O_2CCF_3	7
O_2CMe	8
O_2CCPh	9
$(NPh)_2CH$	10
(N-p-tolyl)$_2$CH)	11
S_2CNEt_2	12
$S_2P(OEt)_2$	13
MeC(O)CHC(O)CMe (acac)	14
MeC(O)CHC(NPh)CMe	15

$$[(\eta^5\text{-Ind})Mo(\eta^3\text{-}C_3H_5)(CO)_2] \xrightarrow[\text{(ii) 2L or } L_2]{\text{(i) } HBF_4/CH_2Cl_2} [(\eta^5\text{-Ind})ML_2(CO)_2]BF_4 + C_3H_6 \quad (2)$$

With the exception of **4**, which could not be isolated as a solid, and the isonitrile derivative **2**, which was only obtained in a rather poor yield from a thick red oil, the cations **1**−**6** are easily isolated as analytically pure crystalline materials. They all present two ν(CO) stretching bands for the *cis*-$(CO)_2$ fragment in their IR spectra. The ^1H NMR characterization was done in CD_2Cl_2 in order to avoid possible solvent-induced indenyl rearrangements. The chemical shifts of the indenyl protons in the η^5 coordination mode assumed for the 18e compounds **1**−**6** follow the typical pattern exemplified in Figure 1a for the well-known case of **1** and are very easy to assign.[18]

Excess $OPPh_3$ and $OP(OMe)_3$ in the respective preparations of **3** and **4** did not change the nature of the final product; *i.e.*, no octahedral product such as $[(\eta^3\text{-Ind})Mo(OPPh_3)_3(CO)_2]BF_4$ or $[(\eta^3\text{-Ind})Mo\{(OP(OMe)_3)_3\}(CO)_2]BF_4$ was formed.

In the case of **2**, two sets of resonances revealed the presence of two isomers. The simplest geometries are represented in **2a**−**c**.

IR data showed that, in the solid state (KBr pellet), only two ν(CO) and two ν(CN) vibrations were present, therefore ruling out the isomer **2c** with a trans arrangement of both CO and CNR ligands. When a sample of solid crystalline **2** was dissolved at −70 °C in CD_2Cl_2, only one set of resonances was present in the ^1H NMR

(17) Casey, C. P.; O'Connor, J. M. *Organometallics* **1985**, *4*, 384.
(18) Ascenso, J. R.; Gonçalves, I. S.; Herdtweck, E.; Romão, C. C. *J. Organomet. Chem.* **1996**, *508*, 169.
(19) (a) Markham, J.; Menard, K.; Cutler, A. *Inorg. Chem.* **1985**, *24*, 1581. (b) Almeida, J. M.; Gonçalves, I. S.; Romão, C. C. *An. Quim. Int. Ed.* **1997**, *93*, 8. (c) Azevedo, C. G.; Calhorda, M. J.; Carrondo, M. A. A. F. d. C. T.; Dias, A. R.; Duarte, M. T.; Galvão, A. M.; Gamelas, C. A.; Gonçalves, I. S.; Piedade, F. M.; Romão, C. C. *J. Organomet. Chem.* **1997**, *544*, 257.

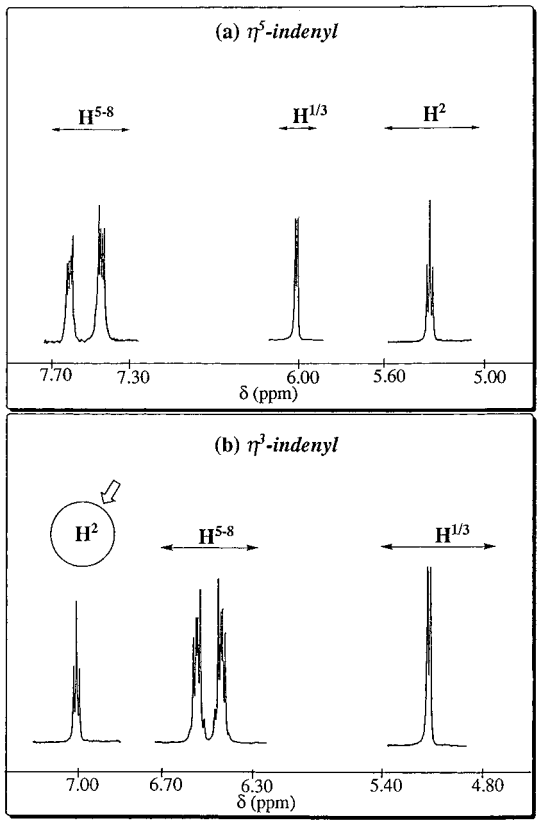

Figure 1. Typical resonances for coordinated indenyl in the complexes $[(\eta^5\text{-Ind})MoL_2(CO)_2]^{0,+}$ (a) and $[(\eta^3\text{-Ind})MoL_3(CO)_2]^{0,+}$ (b).

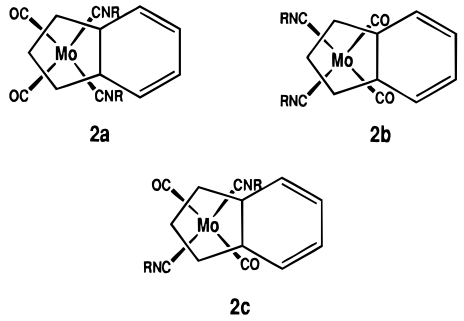

spectrum. Warming to room temperature slowly allowed the appearance of the second isomer until a 1:1 equilibrium ratio was attained. No changes were detected in the resonances of the first isomer. These data are compatible with the presence of only one isomer in the solid state, which was shown to be **2a** on the basis of a crystal structure investigation (Figure 2, Table 1).

Bond distances and angles together with the characteristic slip parameters are listed in Table 1. The compound (Figure 2) is monomeric and belongs to the general family of four-legged piano-stool compounds (Ind/Cp)MoL_4. The geometry around the metal atom is a pseudo square pyramid with the centroid (C11−C17a) in the apical position. All intramolecular distances and angles are in the expected ranges and show no particularities. In general, the observed values for the ring-slippage parameters for **2a** are consistent with those given in the literature[9,18] and are typical for the η^5 coordination of the C5 ring of the indenyl ligand. Detailed analysis of the observed distortions are handicapped by the quality of the crystal data **2a**. However,

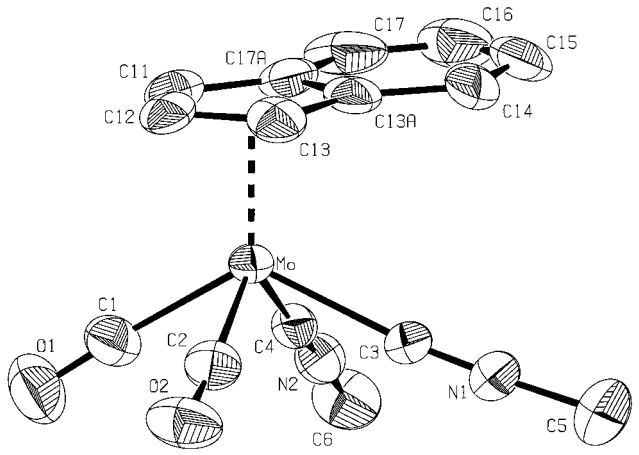

Figure 2. ORTEP plot of the $[(\eta^5\text{-Ind})Mo(CNMe)_2(CO)_2]^+$ cation (**2a**) with the atomic numbering scheme. Thermal ellipsoids are drawn at the 50% probability level. The BF_4^- anion is disordered in two positions.

Table 1. Selected Interatomic Distances (pm), Angles (deg), and Slip Parameters for $[(\eta^5\text{-Ind})Mo(CNMe)_2(CO)_2]BF_4$ (2a)

Mo−C(11)	230.2(9)	Mo−C(13A)	239.3(8)
Mo−C(12)	228.2(8)	Mo−C(17A)	240.0(7)
Mo−C(13)	230.2(8)		
C(11)−C(12)	141.8(14)	C(13A)−C(17A)	142.1(15)
C(11)−C(17A)	141.7(14)	C(14)−C(15)	136.3(16)
C(12)−C(13)	141.0(15)	C(15)−C(16)	141(3)
C(13)−C(13A)	144.3(12)	C(16)−C(17)	132(2)
C(13A)−C(14)	143.3(15)	C(17)−C(17A)	141.8(13)
Mo−C(1)	199.7(11)	Mo−C(3)	212.9(8)
Mo−C(2)	197.8(8)	Mo−C(4)	211.9(8)
C(1)−Mo−C(2)	75.3(4)	C(2)−Mo−C(3)	78.7(3)
C(1)−Mo−C(4)	76.4(4)	C(3)−Mo−C(4)	76.9(3)
$\Delta = \lvert S \rvert$, pm	13.1	Δ(M−C), pm	10
σ, deg	0.4	Ω, deg	3.9
Ψ, deg	3.8		

the allyl-ene distortion is obvious and is shown by the small but definite values of Δ(M−C) of 10 pm for **2a**. A typical alternation of shorter and longer C−C distances in the benzene part of the indenyl ligand indicates diene character (Table 1).

As seen in Figure 2, the solid-state structure displays the isomer **2a**. Theoretical studies (EHMO and DFT calculations) also predict the higher stability of **2a** in comparison to **2b,c** (see below).

The neutral complexes of Chart 3 were similarly characterized by elemental analysis, IR (two ν(CO) stretches), and ^{1}H NMR (typical pattern of Figure 1a for the indenyl resonances).

The trifluoroacetate (**7**) and the acetate (**8**) derivatives are rather labile, as shown by the appearance of more than two CO stretching bands in their IR spectra in KBr pellets. The ^{1}H NMR spectrum of **7** in CD_2Cl_2 at room temperature presents the typical resonances expected for a η^5-Ind complex of this family: two multiplets for H^{5-8} (δ 7.48−7.45 and 7.40−7.30 ppm), a doublet for $H^{1/3}$ (δ 5.94 ppm), and a triplet for H^2 (δ 5.45 ppm). Therefore, a bidentate coordination (κ^2-O_2CCF_3) is assumed. The β-keto(phenyliminato) derivative **15** is exceedingly moisture sensitive, cleanly producing the β-diketonato (acac) congener **14** on hydrolysis in wet solvents (^{1}H NMR evidence).

In a previous publication we reported that the tridentate ligand Me_3tacn (1,4,7-trimethyl-1,4,7-triazacyclononane) adds to $[(\eta^5\text{-Ind})Mo(NCMe)_2(CO)_2]BF_4$ (**1**) to give $[(\eta^3\text{-Ind})Mo(\kappa^3\text{-Me}_3\text{tacn})(CO)_2]BF_4$.[18] Similarly, ttcn reacts with **1** to give the ring-slipped complex $[(\eta^3\text{-Ind})Mo(\kappa^3\text{-ttcn})(CO)_2]BF_4$ (**16**) in excellent yield. **16** has the expected two ν(CO) vibrations in the IR spectrum, and the resonance pattern for the indenyl is consistent with η^3-Ind coordination, namely the resonance of H^2 at δ 7.26 ppm (see Figure 1b and the discussion below).

Addition Reactions of the $[(\eta^5\text{-Ind})ML_2(CO)_2]^{0,+}$ Complexes. As mentioned in the Introduction, dissolution of **1** in NCMe readily forms the adduct **17** as shown in eq 3.[18]

$$[(\eta^5\text{-Ind})Mo(NCMe)_2(CO)_2]BF_4 \underset{CH_2Cl_2}{\overset{NCMe}{\rightleftharpoons}} [(\eta^3\text{-Ind})Mo(NCMe)_3(CO)_2]BF_4 \quad (3)$$

1 **17**

This process is conveniently followed by in situ ^{1}H NMR in $NCCD_3$ and was studied for the cationic and neutral complexes **1**−**15** in order to ascertain the generality and possible dependence of the ring-slippage reaction on the nature of the ligand L. The complexes **1**−**15** were dissolved in $NCCD_3$ at low temperature (ca. −30 °C) and their spectra immediately recorded. The spectral changes were then followed with time, upon temperature increase, or both. In this family of compounds, the resonance pattern of the indenyl ligand in both η^5 and η^3 coordination modes is rather distinctive, as shown in Figure 1 for the typical case of **1** (Figure 1a) and **17** (Figure 1b),[18,19] and allows the facile monitoring of the formation of the adducts of type $[(\eta^3\text{-Ind})MoL_2(NCCD_3)(CO)_2]^{0,+}$ without the need to isolate the compounds. Particularly informative is the highly deshielded H^2 resonance at ca. δ 7.2 ppm, which was taken as the spectral signature of the η^3-Ind coordination in this family of compounds. In the η^5-Ind coordination this triplet appears at ca. δ 5.5 ppm. The spectral data for each compound are given in the Experimental Section.

The ^{1}H NMR spectrum of $[(\eta^5\text{-Ind})Mo(OPPh_3)_2(CO)_2]BF_4$ (**3**) in $NCCD_3$ at −30 °C is compatible with this structural formulation. The doublet at δ 6.58 ppm and the triplet at δ 5.51 ppm are typical of the η^5 coordination mode of the indenyl. After 2 h at this temperature only the adduct $[(\eta^3\text{-Ind})Mo(OPPh_3)_2(NCCD_3)(CO)_2]BF_4$ (**18**) is present in solution, as indicated by the triplet at δ 7.23 ppm, assigned to H^2 of the η^3-Ind ligand of **18**.

In contrast, the ^{1}H NMR spectrum of **4**, in $NCCD_3$ at −30 °C after 3 h still shows the presence of a mixture of the initial η^5 species **4** and the ring-slipped adduct $[(\eta^3\text{-Ind})Mo\{OP(OMe)_3\}_2(NCCD_3)(CO)_2]BF_4$ (**19**). The spectrum of a freshly prepared solution of **2** at −30 °C in $NCCD_3$ is consistent with the exclusive presence of the isomer **2a**. After ca. 2 h two isomers (**2a** and **2b**) are present in a 1:1 ratio, but no sign of addition of NCMe to **2**, with concomitant ring slippage, was observed. This strongly contrasts with the reactivity of the isomeric nitrile complex described in eq 3. Treatment of **2** with excess CNMe (200 μL, 4.2 mmol), in $(CD_3)_2CO$, also fails to give the putative ring-slipped adduct $[(\eta^3\text{-Ind})Mo(CNMe)_3(CO)_2]BF_4$. Under more forcing conditions, reaction of **2** with a 10-fold excess of CNMe in CH_2Cl_2 at room temperature led to the loss of CO (IR evidence). The essential transformations reported so far are included in Schemes 1 and 2, which also summarize the results reported in this paper together with previously reported ones.[18,19]

Scheme 1

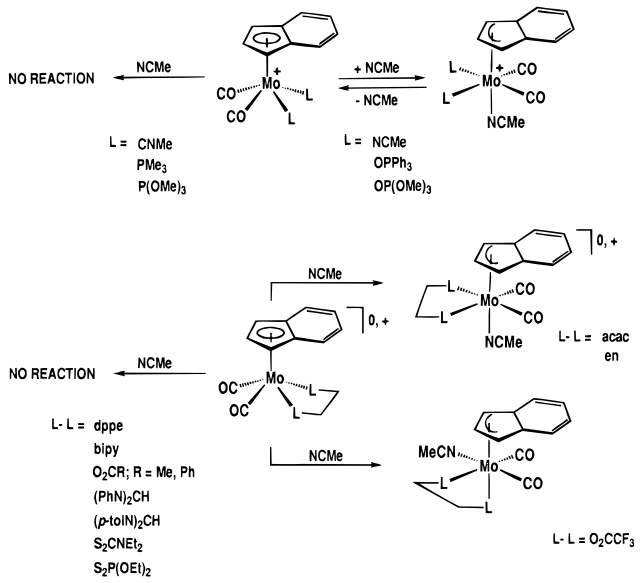

Scheme 2

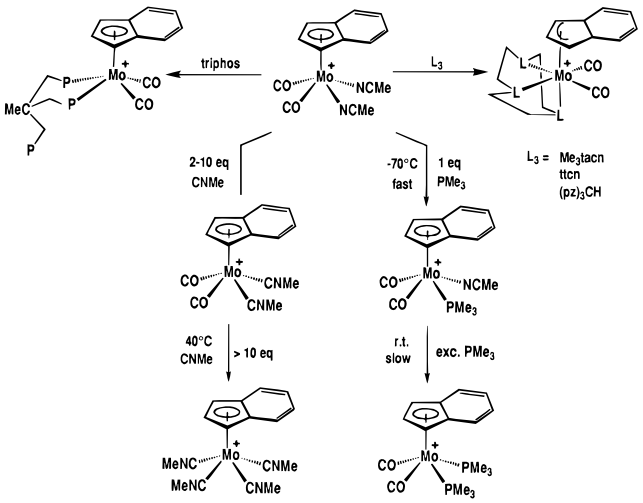

Upon dissolution in $NCCD_3$, the cation $[IndMo\{(PhSCH_2)_2\}(CO)_2]BF_4$ (**4**) readily loses the labile dithioether ligand and forms **17**.

In previous work we have shown that the phosphine cations $[(\eta^5\text{-Ind})Mo(PR_3)_2(CO)_2]^+$ ($PR_3 = {}^1/_3$ triphos, ${}^1/_2$ dppe, PPh_3, PMe_3) add neither NCMe nor a third equivalent of PR_3 to give ring-slipped adducts. However, addition of PR_3 to the cation $[(\eta^5\text{-Ind})Mo(NCMe)_2(CO)_2]^+$ proceeds with overall substitution to give $[(\eta^5\text{-Ind})Mo(PR_3)_2(CO)_2]^+$. This reaction was now monitored by ^{1}H NMR for the case of PMe_3, to try to detect possible intermediates, namely $[(\eta^3\text{-Ind})Mo(NCMe)_2(PMe_3)(CO)_2]^+$, as depicted in Scheme 2.

Addition of 1 equiv of PMe_3 to a solution of $[(\eta^5\text{-Ind})Mo(NCMe)_2(CO)_2]^+$ in CD_2Cl_2 at −70 °C leads to the immediate formation of the substitution product $[(\eta^5\text{-Ind})Mo(NCMe)(PMe_3)(CO)_2]^+$ (**20**). All the starting

materials disappear within ca. 30 min, and no signals are observed in the regions expected for the H^2 resonance of a ring-slipped indenyl ligand. Addition of a second equivalent of PMe_3 at −70 °C did not produce any reaction until the temperature was raised to room temperature. Again, no η^3-Ind species was observed while the resonances of $[(\eta^5\text{-Ind})Mo(PMe_3)_2(CO)_2]^+$ started to replace those of **20**. This second substitution is much slower than the first and only became complete after some hours at room temperature. Further addition of PMe_3 (6 equiv) at room temperature did not produce any change in the Mo complex $[(\eta^5\text{-Ind})Mo(PMe_3)_2(CO)_2]^+$, as previously reported.[18]

The well-resolved ^1H NMR spectrum of the carboxylato complex **7** in CD_2Cl_2 is not reproduced in $NCCD_3$, at room temperature, since only broad signals can be seen, as in the case of the spectrum of $[(\eta^5\text{-Ind})Mo(NCMe)_2(CO)_2]^+$ in the same solvent. At −45 °C the resolution increases and the resonances are assigned in the following way: a broad triplet (δ 7.28 ppm) for H^2, a multiplet (δ 6.46 ppm) for the benzenoid protons H^{5-8}, and two relatively broad peaks (δ 5.19 and 4.76 ppm) for the H^1 and H^3 protons. All these chemical shifts and multiplicities are therefore indicative of the presence of a η^3-indenyl asymmetric complex, for which we propose the structure $[(\eta^3\text{-Ind})Mo(NCMe)(\kappa^2\text{-}O_2CCF_3)(CO)_2]$ (**21**), although NMR cannot clearly rule out a formulation such as $[(\eta^3\text{-Ind})Mo(NCMe)_2(\kappa^1\text{-}O_2CCF_3)(CO)_2]$ due to the impossibility of integrating signals of coordinated $NCCD_3$.

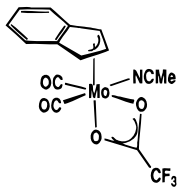

21

Our proposal is supported by the observation that addition of diethyl ether to a solution of **7** in NCMe produces a red-brown crystalline complex which has the same ^1H NMR spectrum, in $NCCD_3$, and the elemental analysis and IR spectrum corresponding to the adduct $[(\eta^3\text{-Ind})Mo(NCMe)(\kappa^2\text{-}O_2CCF_3)(CO)_2]$ (**21**).

After these observations it was quite unexpected to verify that no similar type of addition takes place for the very similar complexes with other carboxylato (**8**, **9**), amidinato (**10**, **11**), dithiocarbamato (**12**), and dithiophosphato (**13**) ligands, in $NCCD_3$. The ^1H NMR spectra of these complexes in $NCCD_3$ between −40 °C and room temperature indicate the typical η^5-indenyl coordination with the H^2 resonance in the range between δ 5.09 ppm (**8**) and δ 5.29 ppm (**12**).

As an exception, the acac derivative $(\eta^5\text{-Ind})Mo(\kappa^2\text{-acac})(CO)_2$ (**14**) readily adds NCMe when dissolved in $NCCD_3$ to give the symmetrical adduct $[(\eta^3\text{-Ind})Mo(\kappa^3\text{-MeCOCHCOMe})(NCMe)(CO)_2]$ (**22**), as in eq 4.

The ^1H NMR spectrum of **22** can only be well-resolved at −45 °C. At this temperature the H^2 triplet appears at δ 7.11 ppm, which represents a downfield shift of ca. 2.10 ppm relative to its chemical shift in the η^5-indenyl coordination of **14** in CD_2Cl_2. An upfield shift of ca. 1.00 ppm is simultaneously recorded for the H^{5-8} protons.

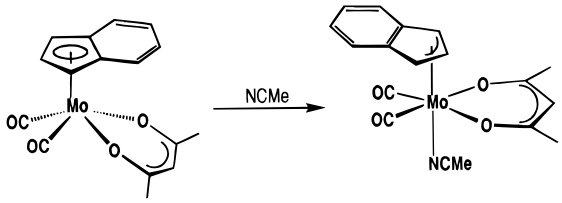

14 **22** (4)

However, this addition is easily reversed and we were not able to isolate **22**.

The enaminone derivative $IndMo\{\kappa^2\text{-MeCOCHC(NPh)Me}\}(CO)_2$ (**15**) also adds NCMe, but less extensively than its acac congener **14**. In fact, the ^1H NMR spectrum of a sample of **15** in $NCCD_3$ shows the presence of the starting material together with the ring-slipped adduct $[(\eta^3\text{-Ind})Mo(NCMe)\{\kappa^2\text{-MeCOCHC(NPh)Me}\}(CO)_2]$ (**23**) after 1 h at −30 °C, and this equilibrium is no longer disturbed at this temperature. Exploratory studies with related enaminones were inconclusive due to their extremely easy hydrolysis to give **14**.

Theoretical Studies

Several theoretical studies have addressed the problem of understanding the electronic structure of indenyl complexes.[6b,10c,20] Faller and co-workers[9] analyzed the structural features of the η^5-indenyl complexes available at the time and concluded that the benzene ring of the indenyl is oriented trans to the ligand exhibiting the greater trans influence.

Our purpose is to understand the structural preferences of η^5- and η^3-indenyl complexes of the types $[(\eta^5\text{-Ind})ML_2(CO)_2]^+$ and $[(\eta^3\text{-Ind})ML_2L'(CO)_2]^+$ and the reactivity patterns of the η^5-indenyl complexes described above. Haptotropic rearrangements of cyclopentadienyl groups and other polyenes started to be theoretically studied long ago, but a considerable amount of new experimental results is now available.[21] Extended Hückel[22] and density functional theory (DFT)[23] calculations will be used.

Bonding in Indenyl Complexes. The indenyl ligand differs from the simpler cyclopentadienyl ligand by the larger number of π orbitals. Those having lower energies are shown in Chart 4, and the notation is that used in ref 20a.

The lower energy orbital, $1\pi_s$, resembles the corresponding one for the Cp and is unique. However, for each orbital belonging to the Cp 1e set, there are two for the indenyl, namely $2\pi_s$ and $3\pi_s$, and $1\pi_a$ and $2\pi_a$. This duplication derives from the presence of the adjacent benzene ring, and it can be noted that in $2\pi_s$ there is no contribution from the two carbons in the

(20) (a) Bonifaci, C.; Ceccon, A.; Santi, S.; Mealli, C.; Zoellner, R. W. *Inorg. Chim. Acta* **1995**, *240*, 541. (b) O'Hare, D.; Green, J. C.; Marder, T.; Collins, S.; Stringer, G.; Kakkar, A. K.; Kaltsoyannis, N.; Kuhn, A.; Lewis, R.; Mehnert, C.; Scott, P.; Kurmoo, M.; Pugh, S. *Organometallics* **1992**, *11*, 48.

(21) (a) Anh, N. T.; Elian, M.; Hoffmann, R. *J. Am. Chem. Soc.* **1978**, *100*, 110. (b) Albright, T. A.; Hofmann, P.; Hoffmann, R.; Lillya, C. P.; Dobosh, P. *J. Am. Chem. Soc.* **1983,** *105*, 3396.

(22) (a) Hoffmann, R. *J. Chem. Phys.* **1963**, *39*, 1397. (b) Hoffmann, R.; Lipscomb, W. N. *J. Chem. Phys.* **1962**, *36*, 2179. (c) Ammeter, J. H.; Bürgi, H.-J.; Thibeault, J. C.; Hoffmann, R. *J. Am. Chem. Soc.* **1978**, *100*, 3686.

(23) Parr, R. G.; Yang, W. *Density Functional Theory of Atoms and Molecules*; Oxford University Press: New York, 1989.

Chart 4

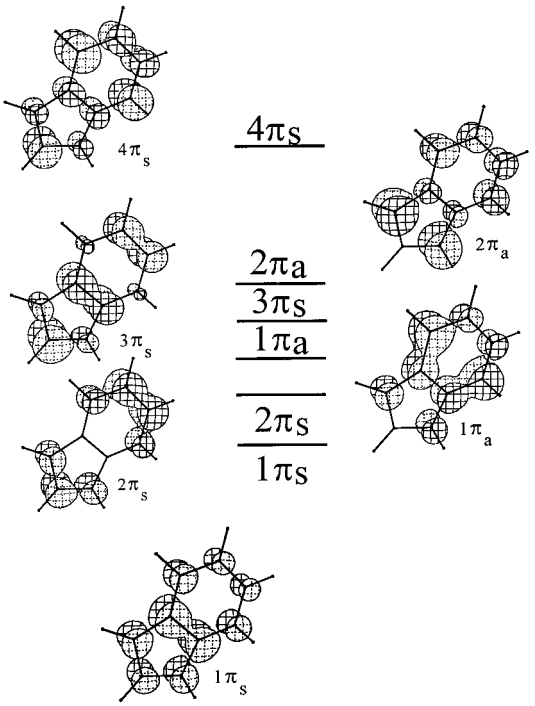

Chart 5

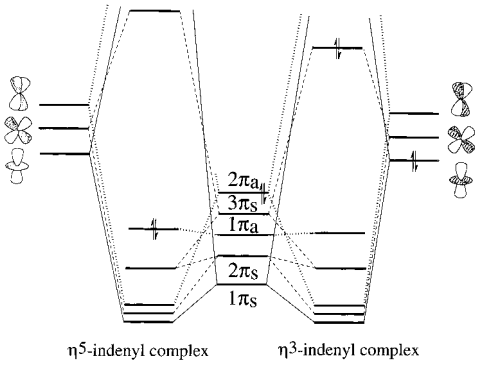

junction, C4 and C9, while in $2\pi_a$ this contribution is very small. The result is that upon bonding to a metal center these orbitals of similar nodal properties will mix.

In a (η^5-Ind)M complex, the ligand formally donates three pairs of electrons to the metal and they come from $1\pi_s$, $2\pi_s$ plus $3\pi_s$ (they mix), and $2\pi_a$ (mixing from $1\pi_a$ is negligible here), interacting with z^2, xz, and yz, respectively (Chart 5, left side). Back-donation is not relevant.

When the indenyl slips and becomes η^3-coordinated due to ligand addition, the metal gains two electrons and one of the previous two-electron stabilizing interactions becomes a four-electron destabilizing interaction. As both the bonding and the antibonding molecular orbitals are populated, one bonding component is lost and only four electrons are formally donated to the metal (see right side of Chart 5). The two lowest, occupied energy d levels for a d^4 metal are not shown in this chart. Notice that the change in the orbitals of the indenyl upon bending does not affect this qualitative picture.

Structural Preferences in Indenyl Complexes. Dft calculations[23,24] were done on [(η^5-Ind)$ML_2(CO)_2$]$^+$

Chart 6

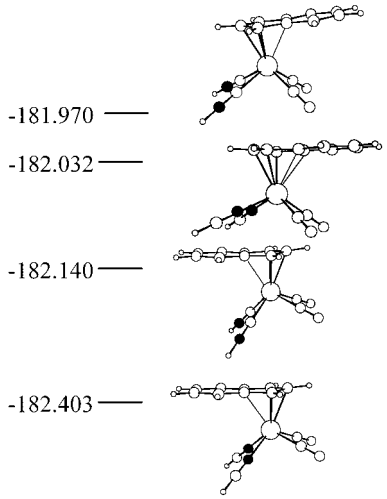

Chart 7

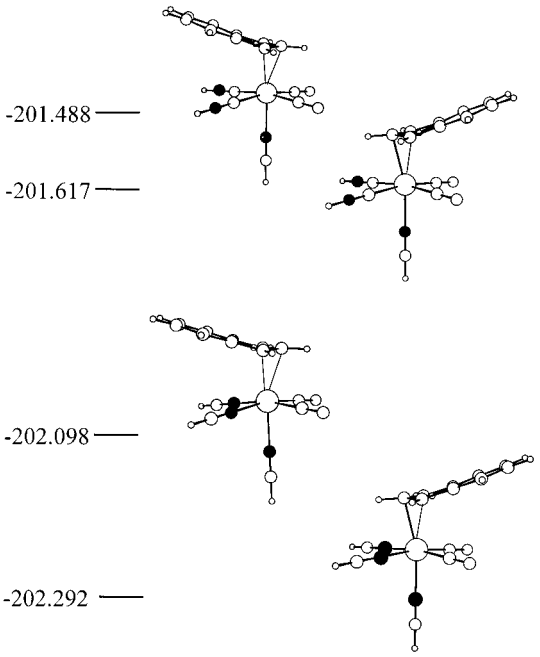

compounds (L = NCH, CNH), showing that the benzene ring preferred, in both cases, to lie trans to the two CO ligands, as seen above in the crystal structure of **2a** and following the rule of thumb of Faller.[9] The energies of these compounds are shown in Chart 6 (eV; black circles indicate N atoms in the nitrile and isonitrile ligands).

Extended Hückel calculations on [(η^5-Ind)$ML_2(CO)_2$]$^+$ (L = NCMe, CNMe) led to the same structural preferences.

DFT calculations were done for the related η^3-indenyl derivatives, namely [(η^3-Ind)Mo $(NCH)_3(CO)_2$]$^+$ (**17**; see eq 3)[18] and the hypothetical isonitrile complex [(η^3-Ind)-Mo $(CNH)_2(NCH)(CO)_2$]$^+$, which might be formed upon addition of NCR to [(η^5-Ind)$M(CNR)_2(CO)_2$]$^+$. The results are depicted in Chart 7 (energy in eV), and as observed in the crystal structure of **17**, the benzene lies cis to the two CO groups; that is, the conformation is not the same as in the η^5-indenyl complexes.

(24) Amsterdam Density Functional (ADF) Program, release 2.01; Vrije Universiteit: Amsterdam, The Netherlands, 1995.

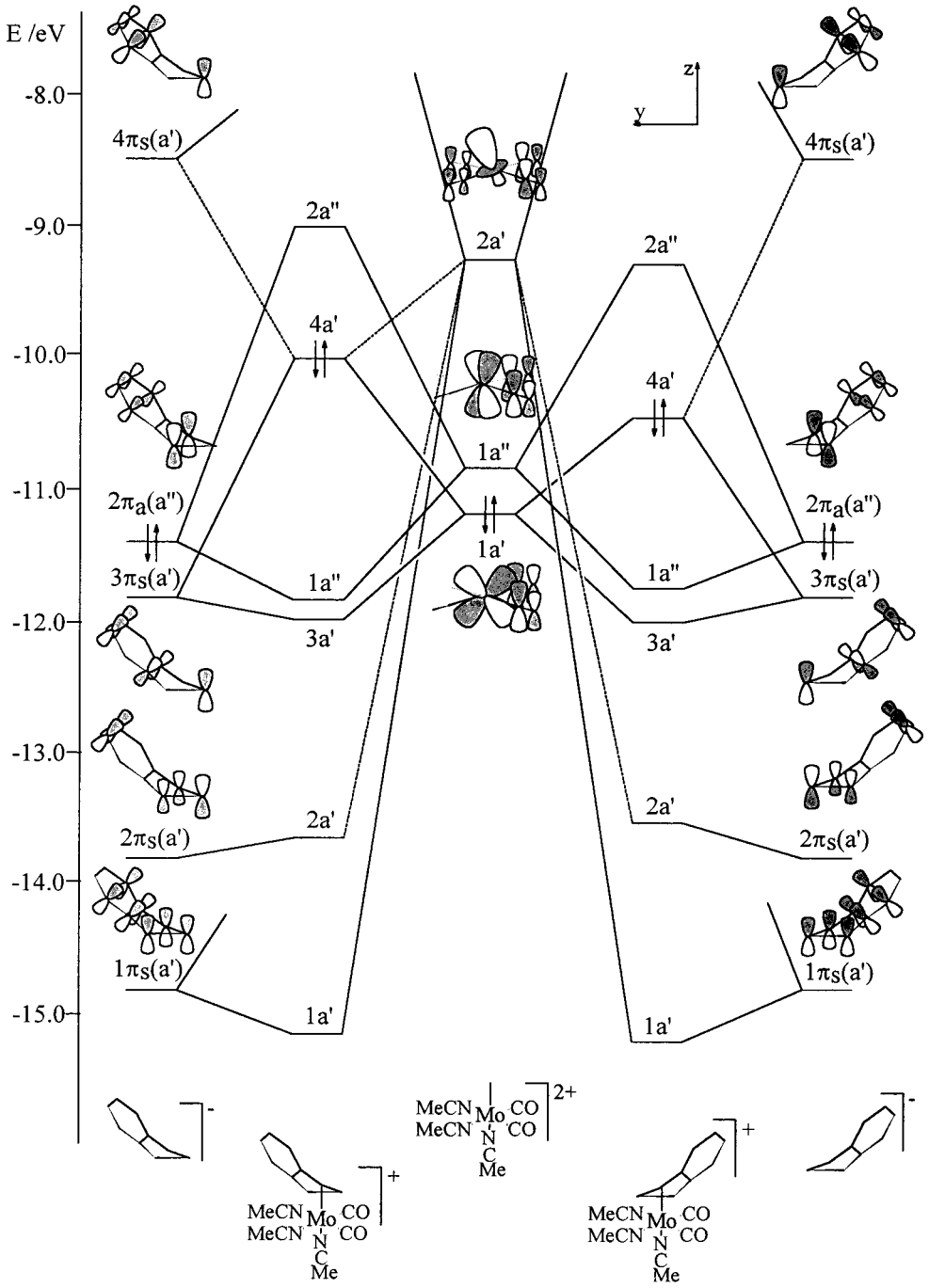

Figure 3. Interaction diagram between a bent η^3-indenyl ligand and the $Mo(NCMe)_3(CO)_2$ fragment for two possible conformations: benzene ring trans (left) or cis (right) to the CO ligands in the model complex $[(\eta^3\text{-Ind})Mo(NCMe)_3(CO)_2]^+$. The lowest energy d level is not shown.

Extended Hückel calculations were performed on the $[(\eta^3\text{-Ind})MoL_2(NCMe)(CO)_2]^+$ (L = NCMe, CNMe, PH_3) model, taking 30° as the folding angle. An optimization of this angle led to a value of 31.5°, not too far from the experimental ones of 24.1 and 27.4° found in the two independent molecules of the W analogue $[(\eta^3\text{-Ind})W(NCMe)_3(CO)_2]^+$.[18] The most stable conformation for L = NCMe, CNMe was the same as in the DFT calculations, but for L = PH_3, the preferred conformation was the opposite (Chart 8).

Chart 8

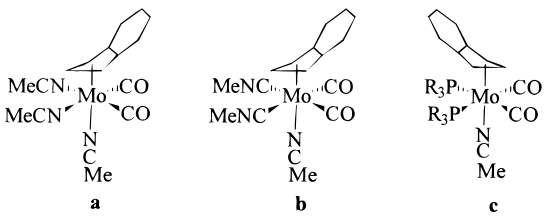

The reason one conformation is preferred can be more easily understood from the EH results. The energy differences between the conformers of the η^3-indenyl derivative are more pronounced than for the η^5-indenyl complex, and it is easier to trace their origin. Our interpretation will be based on the interaction diagram between the η^3-indenyl ligand and the metal fragment $Mo(NCMe)_3(CO)_2$ when they combine in the two limiting orientations, as shown in Figure 3.

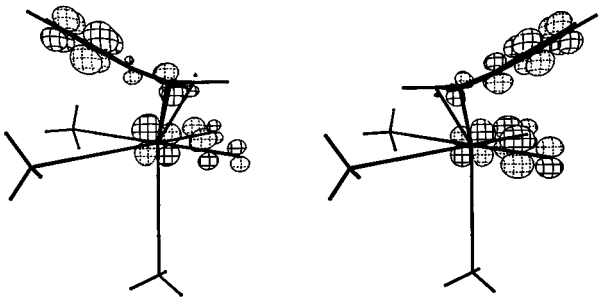

Figure 4. HOMO of $[(\eta^3\text{-Ind})Mo(NCMe)_3(CO)_2]^+$ in two conformations: more stable (right) and less stable (left).

The energy is lower for the conformation shown on the right side, and it reflects the lower energy of the HOMO, which is a metal−indenyl antibonding orbital (remember Chart 5 above) but is also metal−carbonyl bonding. It arises from interaction between *yz* and the $3\pi_s$ orbital. In this molecule, $2\pi_s$ will mix mainly with $1\pi_s$ and interact with the z^2 type orbital. The two HOMOs are shown in Figure 4 in a three-dimensional CACAO picture.[20b] The HOMO for the less favored geometry (left side) is much less Mo−CO bonding.

As pictured in the diagram, the fragment orbitals are exactly the same on the left and on the right. When the bond to the indenyl is established, the metal orbitals must rehybridize in order to achieve a good overlap with the indenyl, and they do it in different ways in the two cases. Notice that, on the right side of the diagram, the most stable isomer, the HOMO comes mostly from 1a′ (∼70%), which is Mo−CO bonding. On the other hand, on the left, a second metal fragment orbital, 2a′, Mo−CO antibonding, mixes in and weakens the Mo−CO bond. The HOMO derives from 1a′ (47%) and from 2a′ (18%). The loss of Mo−CO bonding character accounts for the higher energy and is a consequence of binding the indenyl ligand in this orientation.

A similar picture is found for the hypothetical isomeric ring-slipped adduct $[(\eta^3\text{-Ind})Mo(CNMe)_2NCMe(CO)_2]^+$, where the preferred conformation is still the same, **b** in Chart 8. As the carbonyl is a stronger π-acceptor than the linear isonitrile, the conformation which allows stronger bonding to the strongest π-acceptor is chosen. In the third type of model complex, $[(\eta^3\text{-Ind})Mo(PR_3)_2NCMe(CO)_2]^+$, the same conformation should be chosen on electronic grounds, according to the above arguments, but the bulkiness of the phosphines prevents this arrangement, where the planar allylic group is very close to the phosphines. The rotation of the indenyl group allows the benzene substituent, conveniently bent up, to lie above these bulky ligands (Chart 8, **c**). The preferred conformation predicted for the bis(phosphine) derivative is therefore induced by steric rather than by electronic effects and the bond between the metal and the indenyl ligand is not optimized. This may explain why, as far as we know, there are no examples of $[(\eta^3\text{-Ind})Mo(PR_3)_2(NCMe)(CO)_2]^+$ complexes.

Why do the $[(\eta^5\text{-Ind})MoL_2(CO)_2]^+$ complexes prefer another arrangement with the benzene trans to the CO groups? The energy difference between the two isomers of $[(\eta^5\text{-Ind})Mo(NCMe_2)(CO)_2]^+$ is only 0.14 eV, at the EH level, and is therefore not so easy to trace. The molecular orbital diagram suggests, however, that an electronic situation related to the previous one may be found. The HOMO has a slightly lower energy for the most stable conformer. It originates from a Mo−CO bonding orbital and the corresponding orbital in the η^5-indenyl. The metal fragment has one ligand less, so its frontier orbitals are not exactly the same as those of $MoL_2(CO)_2$, and the four ligands remain farther from the indenyl than in the pseudo-octahedral geometry.

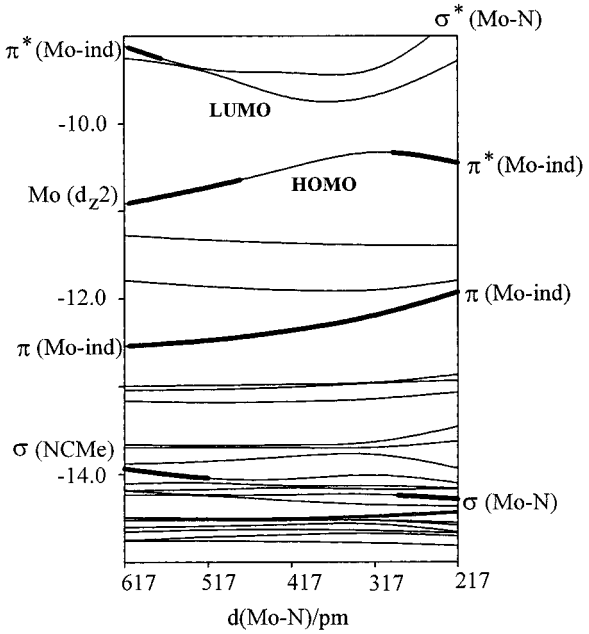

Figure 5. Walsh diagram for the addition of a NCMe ligand to $[(\eta^5\text{-Ind})Mo(NCMe)_2(CO)_2]^+$ to give $[(\eta^3\text{-Ind})Mo(NCMe)_3(CO)_2]^+$.

Ligand Addition Reactions. The reaction of $[(\eta^5\text{-Ind})Mo(NCMe)_2(CO)_2]^+$ with one NCMe was studied initially using extended Hückel calculations, and the main changes of the electronic levels are shown in the Walsh diagram (Figure 5). The significant levels are highlighted and labeled.

The σ lone pair of the nitrile (left side) is stabilized as it becomes the Mo−N bonding orbital and therefore provides the driving force for the reaction. The metal orbital involved in this new Mo−N bond is z^2, which is also the main contributor to the HOMO of the η^5-indenyl complex (left side). It will give rise to the σ^* Mo−N orbital and is very much destabilized, falling outside the energy window shown in Figure 5. As the reaction proceeds, the two electrons which occupied the HOMO of the η^5-indenyl complex (left) will occupy the HOMO of the η^3-indenyl complex (right), which is an orbital mainly located in the metal and in the indenyl and antibonding in character (see Figure 3). This orbital descends from higher energy orbitals on the left and becomes the HOMO after some avoided crossings (no symmetry is kept along the reaction). When the C5 ring of the indenyl bends, going from η^5 to η^3, the two carbon atoms in the junction, C4 and C9, no longer bind to the metal. Thus, the antibonding character of the orbital is greatly relieved. This stabilization of the π^* Mo−Ind orbital upon bending of the ring also contributes to lower the energies of the final state, as can be seen by comparing the energy of the first empty π^* Mo−Ind orbital on each side of the Walsh diagram. The indenyl ligand is forced to bend, along the reaction pathway, to

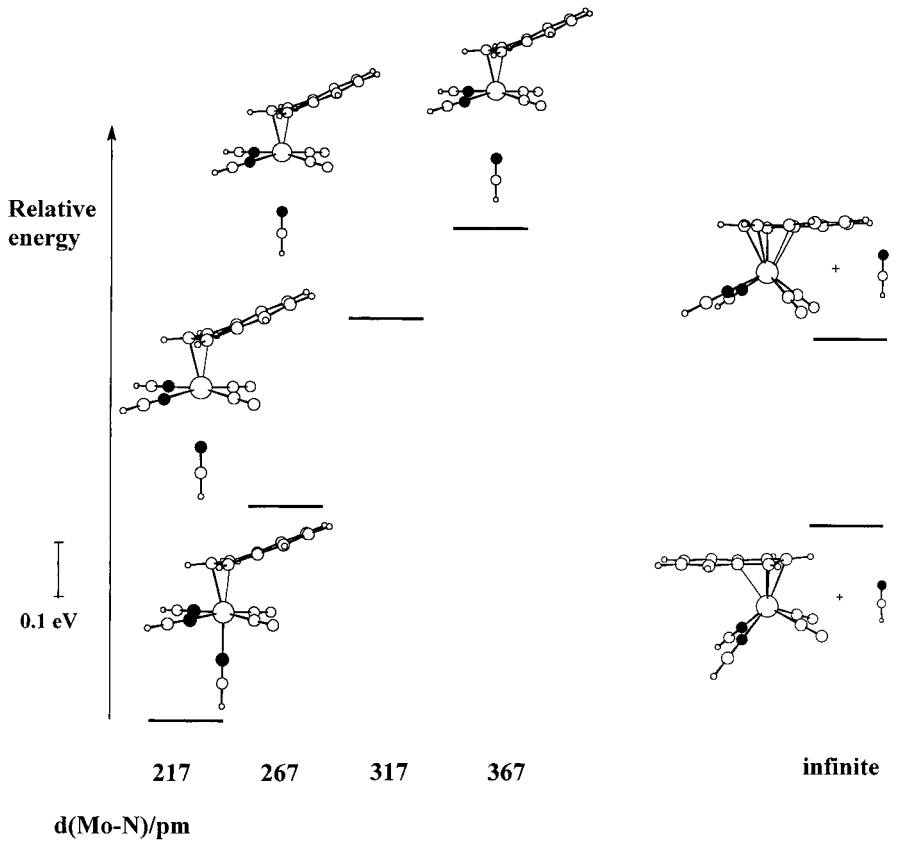

Figure 6. Relative energy when one NCH ligand is moved away from the metal in $[(\eta^3\text{-Ind})MoL_2(NCH)(CO)_2]^+$ and for the final η^5-Ind complex.

provide a more stable HOMO for the resulting complex $[(\eta^3\text{-Ind})Mo(MeCN)_3(CO)_2]^+$.

Finally, the opposite effect, namely the destabilization of the π Mo−Ind levels when the C5 ring bends, can be seen on the level signaled in the Walsh diagram. Here, when two carbon atoms move away from the metal, part of the bonding character is lost and the energy increases. The η^3-indenyl ligand, in the preferred conformation of the final complex, is still strongly bound and therefore the final product is stable. The reaction takes place.

In the related phosphine derivative $[(\eta^5\text{-Ind})Mo(PH_3)_2(CO)_2]^+$, the preferred conformation of the final $[(\eta^3\text{-Ind})Mo(PH_3)_2(NCH)(CO)_2]^+$ derivative should be less favored on electronic grounds. In the presence of bulky ligands, the η^3-indenyl group would be forced to adopt a conformation that prevents a strong bond to the metal (see Chart 8). Therefore, instead of ligand addition accompanied by indenyl slipping, other reactions (or no reaction) will take place. This suggests that the steric effect caused by the bulk of the PR_3 ligands in the starting reagent is responsible for the experimentally observed absence of reaction.

The situation becomes more difficult when $[(\eta^5\text{-Ind})Mo(CNMe)_2(CO)_2]^+$ is considered, because no reaction of nitrile with this complex is observed and steric factors cannot be responsible. There is no difference between CNMe and NCMe from this point of view, and no significant differences could be traced easily at the EH level. This led us to study the starting and final reagents, as well as part of the reaction path, using DFT calculations which provide more reliable energies. We did not attempt to locate a real transition state and find the reaction pathway, as this would be too demanding a calculation owing to the size and absence of symmetry of the system.

With the final product, $[(\eta^3\text{-Ind})MoL_2(NCH)(CO)_2]^+$ with L = NCH or CNH, as starting material, the nitrile was allowed to move away from the metal, as sketched in Figure 6 for L = NCH. A mirror plane was kept along this movement, thereby preventing the indenyl ligand from rotating. It can bend, slip, and change its orientation relative to other ligands. Therefore, the η^3 derivative exhibits the preferred conformation, but the conformation of the final η^5 derivative is not the most stable one.

The energy increases as the ligand moves away from the metal and the molecule rearranges. Eventually the final geometry is reached. The most obvious geometry adjustment taking place is the closing up of the N_{ax}-Mo−N_{eq} angle, which goes from 85.74° (2.17 Å) to 84.39° (2.67 Å), 83.43° (3.17 Å), 82.91° (3.67 Å), and 63.49 Å in the η^5 derivative. At the same time there are small changes in the indenyl ligand, but it remains essentially η^3-coordinated up to a Mo−N distance of 3.67 Å. When L = CNH, the reaction profile is very similar, and the energy increases in a similar way when the Mo−N distance increases. This suggests that the approach of the incoming ligand induces the distortion of the indenyl.

It is also possible to calculate the enthalpy change for reaction 5 from the results of the DFT calculations.

$$[(\eta^5\text{-Ind})MoL_2(CO)_2]^+ + NCH \rightarrow [(\eta^3\text{-Ind})MoL_2(NCH)(CO)_2]^+ \quad (5)$$

Both the starting and the final products are considered

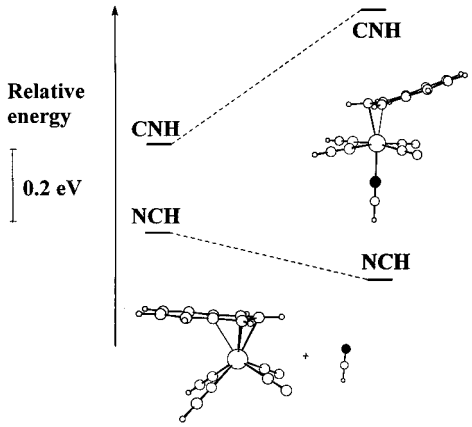

Figure 7. Change in enthalpy for the reaction $[(\eta^5\text{-Ind})MoL_2(CO)_2]^+ + NCH \rightarrow [(\eta^3\text{-Ind})MoL_2(NCH)(CO)_2]^+$.

in their most stable geometry. They are respectively −0.125 eV for L = NCH and 0.416 eV for L = CNH, and this means that while the first reaction is exothermic, the second is endothermic. This result is schematically shown in Figure 7.

The comparison of the energies of the initial and final states indicates that the largest contribution to the global enthalpy change comes from the final η^3 derivative, which is 0.80 eV less stable for the isonitrile complex. The initial η^5 complexes differ only by 0.26 eV, the nitrile complex being again the most stable. This can be explained by the simultaneous presence of two carbonyl ligands trans to both nitriles (or isonitriles). As they are strong π-acceptors, the presence of the nitrile π-donors will make back-donation from the metal relatively efficient, while, on the other hand, isonitriles will compete for the same back-donation. This competition takes place for both η^5 and η^3 complexes, but the electronic balance is more delicate in the η^3 species, where the metal orbitals are also involved in back-donation to the indenyl ring. This competition is responsible for the lower stability of the final product of the reaction when L = CNH, compared to L = NCH.

Discussion and Conclusions

The kinetic rate acceleration of substitution reactions of indenyl complexes vs their cyclopentadienyl congeners has long been attributed to the easy slippage of the indenyl ring from a η^5 to a η^3 coordination mode.[4,5] In view of this mechanistic proposal and the fact that a number of η^3-indenyl complexes are stable entities, one might expect to be able to isolate and characterize η^3-indenyl complexes formed upon ligand addition to η^5-indenyl substrates. However, the number of η^3-indenyl complexes prepared in this way is surprisingly small. The most clear-cut examples result from CO uptake by the very electron rich complexes $[(\eta^5\text{-Ind})Fe(CO)_2]^-$ and $(\eta^5\text{-Ind})_2V$ to give respectively $[(\eta^3\text{-Ind})Fe(CO)_3]^-$ [7b] and $(\eta^5\text{-Ind})(\eta^3\text{-Ind})V(CO)_2$.[7c] The formation of $(\eta^3\text{-Ind})Ir(PMe_3)_3$ from $(\eta^5\text{-Ind})Ir(COD)$ and excess PMe_3 is also a related example.[7a] The search for $(\eta^3\text{-Ind})Re(CO)_3L$ derivatives from $(\eta^5\text{-Ind})Re(CO)_3$ and excess L only led to $(\eta^1\text{-Ind})Re(CO)_3L_2$ (L = $P(^n\text{Bu})_3$, $^1/_2$ bipy).[17] Therefore, the easy addition of NCMe to the cation $[(\eta^5\text{-Ind})M(NCMe)_2(CO)_2]^+$ (M = Mo, W) came as a surprise, for NCMe is a weak, labile donor and the cation is not a particularly electron-rich species. Besides NCMe, similar reactions are observed with DMF and oxygen ligands such as $OPPh_3$ and $OP(OMe)_3$, acac, and en but not with CNMe, PMe_3 and other phosphines, bipy, carboxylates, etc. Although steric considerations may be important in determining this reactivity behavior, their role remains unclear. In this respect, the CNMe case is particularly striking, since we were able to detect neither $[(\eta^3\text{-Ind})M(CNMe)_3(CO)_2]^+$ nor $[(\eta^3\text{-Ind})M(CNMe)_2(NCMe)(CO)_2]^+$. In their studies on the addition/slippage reactions of $[(\eta^7\text{-}C_7H_7)M(CN^t\text{Bu})(CO)_2]^+$ and $[(\eta^5\text{-}C_7H_9)ML_2(CO)_2]^+$ (M = Mo, W) Whiteley and coworkers reported many similar observations.[25] In the first place, NCMe forms adducts with most complexes of both types, e.g. $[(\eta^3\text{-}C_7H_7)M(NCMe)_3(CO)_2]^+$ from $[(\eta^7\text{-}C_7H_7)M(NCMe)(CO)_2]^+$ and $[(\eta^3\text{-}C_7H_9)ML_2(NCMe)(CO)_2]^+$ from $[(\eta^5\text{-}C_7H_9)ML_2(CO)_2]^+$. In the latter example, the reversible adduct formation with NCMe is less favored by L_2 = diphosphines relative to L_2 = bipy. On the other hand, addition of $CN^t\text{Bu}$ to $[(\eta^7\text{-}C_7H_7)M(CN^t\text{Bu})(CO)_2]^+$ leads to associative substitution via $[(\eta^3\text{-}C_7H_7)M(CN^t\text{Bu})_3(CO)_2]^+$ and the similar reaction with $[(\eta^5\text{-}C_7H_9)ML_2(CO)_2]^+$ leads to CO substitution via isolable $[(\eta^3\text{-}C_7H_9)ML_2(CN^t\text{Bu})(CO)_2]^+$. The coordination of a π-acceptor to the metal decreases the ability toward ring slippage because $[(\eta^5\text{-}C_7H_9)M(CNMe)(dppe)(CO)]^+$ is no longer capable of adding NCMe as $[(\eta^5\text{-}C_7H_9)M(dppe)(CO)_2]^+$ does.[25]

All these facts clearly point to the existence of an electronic regulation of the addition/slippage reaction. EHMO calculations correctly predict all the conformational preferences in the four-legged piano-stool species $[(\eta^5\text{-Ind})MoL_2(CO)_2]^+$ and six-coordinated $[(\eta^3\text{-Ind})ML_2L'(CO)_2]^+$ complexes involved, but they are unable to disclose the electronic control of the reaction and associated energy changes. A thermodynamic explanation is, however, provided by DFT calculations on model compounds, i.e. with NCH and CNH instead of NCMe and CNMe. In fact, the indenyl slippage reaction is exothermic for NCH addition and endothermic for CNH addition to $[(\eta^5\text{-Ind})ML_2(CO)_2]^+$ (L = CNH, NCH). Assuming that the entropy of the addition/slippage reaction is negative ($T\Delta S < 0$), the process is only thermodynamically possible for reactions that are exothermic enough to give $\Delta G° < 0$. These energetics seem to be governed mainly by the M−CO bond energy changes that take place during the addition and are dependent on the nature of L. Destabilizing the M−CO bond in the octahedral adduct with competing π-acceptors, e.g. CNMe and bipy, disfavors or prevents the observation of the ring slippage process. Conversely, addition of π-donors such as NCMe and oxygen ligands assists the ring slippage adduct formation by electron donation into the metal orbitals (*yz*, *xz*) that enhance M−CO back-bonding and the π Mo−Ind interaction. Certainly, minor differences between several L ligands may lead to different stabilities of the ring-slipped adducts. The lack of reactivity of the carboxylates $[(\eta^5\text{-Ind})M(O_2CR)(CO)_2]$ (R = Me, Ph) toward NCMe addition contrasts sharply with the extremely facile addition of

(25) (a) Beddoes, R. L.; Hinchliffe, J. R.; Souza, A.−L. A. B.; Whiteley, M. W. *J. Chem. Soc., Dalton Trans.* **1994**, 2303. (b) Hinchliffe, J. R.; Ricalton, A.; Whiteley, M. W. *Polyhedron* **1991**, *10*, 267. (c) Green, M. L. H.; Ng, D. K. P. *Chem. Rev.* **1995**, *95*, 439.

this solvent to the related complexes $[(\eta^5\text{-Ind})ML_2(CO)_2]^+$ (L = acac, CF_3COO).

The combination of our results with those of Whiteley allows for a systematization of the characteristics of the addition/ring slippage reactions in the family of $[(\pi\text{-}C_nH_m)ML_y(CO)_2]^{z+}$ complexes (M = Mo(II), W(II); $\pi\text{-}C_nH_m = \eta^5$-Cp, η^5-Ind, η^5-C_7H_9, η^7-C_7H_7; $y = 1, 2$; $z = 0, 1$). (i) The ease of ring slippage within π-systems increases in the order η^5-Cp < η^5-Ind < η^5-C_7H_9 < η^7-C_7H_7. (ii) NCMe adds reversibly to all these compounds except η^5-Cp. (iii) π-Acceptor ligands L (e.g. CNR) destabilize the formation of ring-slipped adducts with NCMe. (iv) As a result of the preceding observations, reaction with CNR ligands only leads to isolation of ring slipped adducts in the case of η^5-C_7H_9 and η^7-C_7H_7 derivatives; otherwise, overall substitution is observed.

This general picture seems at first glance counterintuitive, for the stronger donors (PMe_3, CNR, bipy, etc.) seem not to favor addition reactions, whereas the weak, labile NCMe promotes ring slippage in all cases except for Cp. However, accumulated kinetic evidence on the indenyl effect as well as the stepwise substitution reactions of $[(\eta^7\text{-}C_7H_7)Mo(CN^tBu)(CO)_2]^+$ and $[(\eta^5\text{-}C_7H_9)Mo(CN^tBu)_2(CO)_2]^+$ with isolable ring-slipped intermediates shows that substitutions are associative and entrain ring slippage. Therefore, the impossibility of observing ring-slipped species such as $[(\eta^3\text{-Ind})ML_2L'(CO)_2]^+$ simply means that they are too energetic and probably very close to the transition state in the respective substitution reactions toward $[(\eta^5\text{-Ind})MLL'(CO)_2]^+$. As revealed by the snapshots taken along the reaction pathway by means of DFT calculations (Figure 6), indenyl slippage is clearly present at very long, almost nonbonding M-NCH distances (3.67 Å). This is more readily interpreted in terms of eq 6.

$$[(\eta^5\text{-Ind})ML_2(CO)_2]^+ \rightleftharpoons [(\eta^3\text{-Ind})ML_2(CO)_2]^+ + L'$$

$$[(\eta^3\text{-Ind})ML_2(CO)_2]^+ + L' \rightarrow [(\eta^3\text{-Ind})ML'_2(CO)_2]^+ \quad (6)$$

$$[(\eta^3\text{-Ind})ML_2L'(CO)_2]^+ \rightarrow [(\eta^5\text{-Ind})MLL'(CO)_2]^+ + L$$

The rapid $\eta^5 \rightleftharpoons \eta^3$ "preequilibrium" gives rise to the electronically unsaturated species $[(\eta^3\text{-Ind})Mo(CO)_2L_2]^{0,+}$, which is intercepted by weak ligands to eventually form stable entities, the ring-slipped adducts, which are "en route" toward the substitution products. Presenting it as an alternative possibility, Basolo and co-workers considered this rapid preequilibrium as totally consistent with the kinetic data on the substitution reaction of $(\eta^5\text{-Ind})Mn(CO)_3$ by phosphines, which can also be interpreted on the basis of the more familiar addition/slippage associative pathway.[4] Strong donors and/or π-acceptors destabilize the ring-slipped adducts and give rapid substitutions (or back-reactions to the starting materials). Also, the nodal characteristics of the different π-systems may subtly influence the stability of the η^3-indenyl derivatives. A more extended π-system will shift the "equilibrium" to the right because the energy of the different hapticities is "smoothed out" and the reaction becomes less discriminative. As a result, the stability of the adducts will increase and they can be observed with stronger donors and/or π-acceptors.

Experimental Section

All preparations and manipulations were done with standard Schlenk techniques under an atmosphere of argon. Solvents were dried by standard procedures (THF, Et_2O, toluene, and hexane over Na/benzophenone ketyl; CH_3COCH_3 over anhydrous K_2CO_3; CH_2Cl_2, NCMe, and triethylamine over CaH_2), distilled under argon, and kept over 4 Å molecular sieves (3 Å for NCMe).

Microanalyses were performed at the ITQB. ^1H and ^{13}C spectra were measured on a Bruker CXP 300 and on a Bruker AMX 300. ^1H chemical shifts are reported on the scale relative to $SiMe_4$ (δ 0.0). Infrared spectra were obtained using a Unicam Mattson Mod 7000 FTIR spectrometer.

The following reagents were prepared as published: IndMo(η^3-C_3H_5)$(CO)_2$,[7e,f] $(PhSCH_2)_2$,[26] CpMo(η^3-C_3H_5)$(CO)_2$,[7e,f] [IndMoI$(CO)_2]_2$,[7e,f] *N,N′*-diphenylformamidine ([HC(NPh)(NHPh)]),[27] the silver derivative of *N,N′*-diphenylformamidine (Ag{HC$(NPh)_2$}),[28] *N,N′*-di-*p*-tolylformamidine ([HC(HN-*p*-tolyl)(N-*p*-tolyl)]),[29] 4-anilinopent-3-en-2-one (MeCOCHC(NHPh)Me),[30,31] triphenylphosphine oxide ($OPPh_3$),[32] [IndMo$(NCMe)_2(CO)_2$]BF_4,[7e,f] and CNMe.[33]

The silver derivative of *N,N′*-di-*p*-tolylformamidine (Ag{HC$(N\text{-}p\text{-tolyl})_2$}) resulted from a preparation similar to that for Ag{HC$(NPh)_2$}. The lithium salt of 4-anilinopent-3-en-2-one (Li{MeCOCHC(NPh)Me}) was prepared by adding a 1.6 M solution of *n*-butyllithium in ether (1 equiv) to a cold solution (−70 °C) of the enaminone in THF.

Preparation of [IndMo(CNMe)$_2$(CO)$_2$]BF$_4$ (2). A solution of IndMo(η^3-C_3H_5)$(CO)_2$ (0.20 g, 0.65 mmol) in CH_2Cl_2 (20 mL) was treated with $HBF_4{\cdot}Et_2O$ (1 equiv). After 10 min, CNMe was added (61 μL, 1.30 mmol) and the reaction continued for 1 h at room temperature. After concentration to ca. 5 mL and addition of ether, a yellow microcrystalline product precipitated, mixed with a dark oil. This was further recrystallized from CH_2Cl_2/Et_2O to give the pure compound in 40% yield. Anal. Found: C, 41.33; H, 3.04; N, 6.66. Calcd for $C_{15}H_{13}BF_4N_2O_2Mo$: C, 41.32; H, 3.00; N, 6.42. Selected IR (KBr, cm^{-1}): 2228, 2214, vs, ν(CN); 1995, 1927, vs, ν(CO). ^1H NMR ($NCCD_3$, 300 MHz, −40 °C, δ in ppm): isomer A, 7.67−7.64 (m, 2H, H^{5-8}), 7.35−7.32 (m, 2H, H^{5-8}), 6.22 (d, 2H, $H^{1/3}$), 5.47 (t, 1H, H^2), 3.44 (s, 6H, Me); isomer B, 7.63−7.59 (m, 2H, H^{5-8}), 7.28−7.25 (m, 2H, H^{5-8}), 6.11 (d, 2H, $H^{1/3}$), 5.61 (t, 1H, H^2), 3.59 (s, 6H, Me).

Preparation of [IndMo(OPPh$_3$)$_2$(CO)$_2$]BF$_4$ (3). A solution of IndMo(η^3-C_3H_5)$(CO)_2$ (0.20 g, 0.65 mmol) in CH_2Cl_2 (20 mL) was treated with $HBF_4{\cdot}Et_2O$ (1 equiv). After 10 min, excess $OPPh_3$ was added (0.39 g, 1.40 mmol) and the reaction continued for 2 h at room temperature. After concentration to ca. 5 mL and addition of ether, a dark orange microcrystalline product precipitated. This was further recrystallized from CH_2Cl_2/Et_2O to give the pure compound in 90% yield. Anal. Found: C, 61.49; H, 4.51. Calcd for $C_{47}H_{37}BF_4O_4P_2Mo$: C, 62.00; H, 4.10. Selected IR (KBr, cm^{-1}): 1942, 1852, vs, ν(CO); 1120, ν(P═O). ^1H NMR ($NCCD_3$, 300 MHz, −30 °C, after 1 h, δ in ppm): [(η^5-Ind)Mo$(OPPh_3)_2(CO)_2$]BF_4, 7.63−7.49 (m, 30H, Ph), 7.10−7.05 (m, 2H, H^{5-8}), 6.86 (m (br), 2H,

(26) Hartley, F. R.; Murray, S. G.; Levason, W.; Soutter, H. E.; McAuliffe, C. A. *Inorg. Chim. Acta* **1979**, *35*, 265.
(27) Giacolone, A. *Gazz. Chim. Ital.* **1932**, *62*, 577.
(28) Bradley, W.; Wright, I. *J. Chem. Soc.* **1956**, 640.
(29) Backer, H. J.; Wanmaker, W. L. *Recl. Trav. Chim. Pays-Bas* **1949**, *68*, 247.
(30) Collman, J. P.; Kittleman, E. T. *Inorg. Chem.* **1962**, *1*, 499.
(31) Iida, H.; Yuasa, Y.; Kibayashi, C.; Iitaka, Y. *J. Chem. Soc., Dalton Trans.* **1956**, 640.
(32) Gilman, H.; Brown, G. E. *J. Am. Chem. Soc.* **1945**, *67*, 824.
(33) Schuster, R. E.; Scott, J. E.; Casanova, J., Jr. *Org. Synth.* **1966**, *46*, 76.

H^{5-8}), 6.58 (d, 2H, $H^{1/3}$), 5.51 (t, 1H, H^2); [(η^3-Ind)Mo($OPPh_3$)$_2$-**(NCMe)**$(CO)_2$]BF_4, 7.63−7.49 (m, 30H, Ph), 7.23 (t, 1H, H^2), 6.50−6.47 (m, 2H, H^{5-8}), 6.42−6.39 (m, 2H, H^{5-8}), 5.12 (d, 1H, H^2). ^{1}H NMR ($NCCD_3$, 300 MHz, −30 °C, after 2h, δ in ppm): [(η^3-Ind)Mo($OPPh_3$)$_2$**(NCMe)**$(CO)_2$]BF_4, 7.64−7.47 (m, 30H, Ph), 7.23 (t, 1H, H^2), 6.50−6.47 (m, 2H, H^{5-8}), 6.42−6.39 (m, 2H, H^{5-8}), 5.12 (d, 2H, $H^{1/3}$).

Preparation of [IndMo{OP(OMe)$_3$}$_2$(CO)$_2$]BF_4 (4). A solution of IndMo(η^3-C_3H_5)$(CO)_2$ (0.20 g, 0.65 mmol) in CH_2Cl_2 (20 mL) was treated with HBF_4·Et_2O (1 equiv). After 10 min, excess $OP(OMe)_3$ was added (0.16 mL, 1.40 mmol) and the reaction continued for 2 h at room temperature. After concentration to ca. 5 mL and addition of ether, a reddish brown oil precipitates in ca. 90% yield. Several attempts to solidify the compound by dissolving it in CH_2Cl_2 and slowly adding of Et_2O or by washing it with hexane and ether failed to yield the solid compound. Selected IR (KBr, cm^{-1}): 1956, 1873, vs, ν(CO); 1244, ν(P═O). ^{1}H NMR ($NCCD_3$, 300 MHz, −30 °C, δ in ppm): [(η^5-Ind)Mo{$OP(OMe)_3$}$_2$$(CO)_2$]$BF_4$, 7.81−7.78 (m, 2H, H^{5-8}), 7.64−7.61 (m, 2H, H^{5-8}), 6.18 (d, 2H, $H^{1/3}$), 5.02 (t, 1H, H^2), 3.68 (s, 6H, Me); [(η^3-Ind)Mo{$OP(OMe)_3$}$_2$-**(NCMe)**$(CO)_2$]BF_4, 7.22 (t, 1H, H^2), 6.47−6.40 (m, 4H, H^{5-8}), 5.12 (d, 2H, $H^{1/3}$), 3.68 (s, 6H, Me).

Preparation of [IndMo{(κ^2-PhSCH$_2$)$_2$}(CO)$_2$]BF_4 (6). A solution of IndMo(η^3-C_3H_5)$(CO)_2$ (0.20 g, 0.65 mmol) in CH_2Cl_2 (20 mL) was treated with HBF_4·Et_2O (1 equiv). After 10 min, $PhSCH_2CH_2SPh$ was added (0.18 g, 0.75 mmol) and the reaction left for 1 h at room temperature. After concentration to ca. 5 mL and addition of ether, an orange product precipitated. This was further recrystallized from CH_2Cl_2/Et_2O to yield the pure compound in 95% yield. Anal. Found: C, 49.84; H, 3.48. Calcd for $C_{25}H_{21}BF_4O_2S_2Mo$: C, 49.83; H, 3.52. Selected IR (KBr, cm^{-1}): 1983, 1912, vs, ν(CO). ^{1}H NMR (CD_2Cl_2, 300 MHz, room temperature, δ in ppm): 7.55−7.48 (m, 10H, Ph); 7.41−7.38 (m, 4H, H^{5-8}), 6.13 (d, 2H, $H^{1/3}$), 5.20 (t, 1H, H^2), 2.55 (m, 2H, CH_2), 1.99 (m, 2H, CH_2).

Preparation of IndMo(κ^2-OOCCF$_3$)(CO)$_2$ (7). A solution of IndMo(η^3-C_3H_5)$(CO)_2$ (0.22 g, 0.71 mmol) in CH_2Cl_2 (15 mL) was treated with excess CF_3COOH. After 2 h the solution was taken to dryness and the residue was washed at low temperature with hexane/pentane. The dark red microcrystalline complex was isolated in 98% yield. Anal. Found: C, 41.24; H, 1.75. Calcd for $C_{13}H_7F_3O_4Mo$: C, 41.08; H, 1.86. Selected IR (KBr, cm^{-1}): 1971, 1960, 1904, 1886, vs, ν(CO), 1672 ν(C═O). ^{1}H NMR (CD_2Cl_2, 300 MHz, room temperature, δ in ppm): 7.48−7.45 (m, 2H, H^{5-8}), 7.40−7.30 (m, 2H, H^{5-8}), 5.94 (d, 2H, $H^{1/3}$), 5.45 (t, 1H, H^2).

Preparation of IndMo(κ^2-OOCMe)(CO)$_2$ (8). A solution of IndMo(η^3-C_3H_5)$(CO)_2$ (0.20 g, 0.65 mmol) in CH_2Cl_2 (15 mL) was treated with HBF_4·Et_2O (1 equiv). After 10 min excess anhydrous sodium acetate was added (0.06 g, 0.75 mmol) and the reaction continued for 5 h, after which time the mixture was filtered and the resulting solution taken to dryness. The oily residue was washed with a small portion of cold hexane and then efficiently extracted with Et_2O to give the dark red microcrystalline complex in 90% yield. The product was further recrystallized overnight from Et_2O/hexane (1/3) at −30 °C. Anal. Found: C, 48.27; H, 3.22. Calcd for $C_{13}H_{10}O_4Mo$: C, 47.87; H, 3.09. Selected IR (KBr, cm^{-1}): 1956, 1867, 1844, vs, ν(CO); 1512. ^{1}H NMR ($NCCD_3$, 300 MHz, −40 °C, δ in ppm): 7.45−7.42 (m, 2H, H^{5-8}), 7.39−7.36 (m, 2H, H^{5-8}), 6.24 (d, 2H, $H^{1/3}$), 5.09 (t, 1H, H^2), 1.48 (s, 3H, Me).

Preparation of IndMo(κ^2-OOCPh)(CO)$_2$ (9). A solution of IndMo(η^3-C_3H_5)$(CO)_2$ (0.20 g, 0.65 mmol) in CH_2Cl_2 (15 mL) was treated with HBF_4·Et_2O (1 equiv). After 10 min excess anhydrous sodium benzoate (0.11 g, 0.75 mmol) was added and the reaction continued for 5 h, after which time the mixture was filtered and the resulting solution taken to dryness. The oily residue was washed with a small portion of cold hexane and then very efficiently extracted with Et_2O to give a dark red microcrystalline complex in 90% yield. The product was further recrystallized from ether/hexane (1/3) by prolonged cooling at −30 °C. Anal. Found: C, 55.79; H, 3.16. Calcd for $C_{18}H_{12}O_4Mo$: C, 55.69; H, 3.11. Selected IR (KBr, cm^{-1}): 1956, 1863, vs, ν(CO); 1601, 1501. ^{1}H NMR ($NCCD_3$, 300 MHz, −40 °C, δ in ppm): 7.58 (d(br), 2H, Ph), 7.50−7.48 (m, 2H, H^{5-8}), 7.33 (c, 3H, Ph), 7.16−7.14 (m, 2H, H^{5-8}), 6.34 (d, 2H, $H^{1/3}$), 5.18 (t, 1H, H^2). ^{13}C{^{1}H} NMR ($NCCD_3$, 75 MHz, room temperature, δ in ppm): 248.28, CO; 133.82, 129.85, 129.05, 126.89, 94.00, 78.08.

Preparation of IndMo{κ^2-HC(NPh)$_2$}(CO)$_2$ (10). A solution of IndMo(η^3-C_3H_5)$(CO)_2$ (0.20 g, 0.65 mmol) in CH_2Cl_2 (15 mL) was treated with HBF_4·Et_2O (1 equiv). After 10 min ^{n}Bu$_4$NI (0.25 g, 0.70 mmol) was added and the reaction continued for 1 h. The complex $[IndMo(CO)_2I]_2$ was isolated as described in the literature[7f] and dissolved in CH_2Cl_2 (20 mL). A slight excess of Ag{$HC(NPh)_2$} (0.21 g, 0.70 mmol) was added, and after 10 h of stirring at room temperature, the AgI precipitate was filtered and the solution taken to dryness. The obtained residue was efficiently extracted with hexane and an orange powder separated by concentration of the extract solution. Yield: 60%. Anal. Found: C, 61.95; H, 4.01; N, 6.16. Calcd for $C_{24}H_{18}N_2O_2Mo$: C, 62.35; H, 3.92; N, 6.06. Selected IR (KBr, cm^{-1}): 1939, 1850, vs, ν(CO). ^{1}H NMR ($NCCD_3$, 300 MHz, −40 °C, δ in ppm): 8.31 (s, 1H, CH), 7.28−7.23 (m, 2H, H^{5-8}), 7.10−7.07 (m, 2H, H^{5-8}), 7.00−6.94 (c, 10H, Ph), 6.32 (s (br), 2H, $H^{1/3}$), 5.22 (t, 1H, H^2). ^{13}C{^{1}H} NMR ($NCCD_3$, 75 MHz, room temperature, δ in ppm): 237.34, CO; 151.55, CH; 146.16, Ph (C^1); 130.46, $C^{5/8}$; 128.90, Ph($C^{3/5}$); 128.48, $C^{6/7}$; 124.18, Ph (C^4); 122.01, $C^{4/9}$; 119.62, Ph ($C^{2/6}$); 80.13, C^2; 77.31, $C^{1/3}$.

Preparation of IndMo{κ^2-HC(N-*p*-tolyl)$_2$)}(CO)$_2$ (11). This complex is prepared by a process entirely similar to that for IndMo{$HC(NPh)_2$}$(CO)_2$ using a slight excess of Ag{HC(N-*p*-tolyl)$_2$} (0.23 g, 0.70 mmol). Yield: 60%. Anal. Found: C, 63.85; H, 4.54; N, 5.91. Calcd for $C_{26}H_{22}N_2O_2Mo$: C, 63.68; H, 4.52; N, 5.71. Selected IR (KBr, cm^{-1}): 1946, 1854, 1840 vs, ν(CO). ^{1}H NMR ($NCCD_3$, 300 MHz, −40 °C, δ in ppm): 8.22 (s, 1H, CH), 7.09−7.04 (d (br), 6H, tolyl +$H^{5/8}$), 6.98−6.94 (m, 2H, $H^{5/8}$), 6.67−6.64 (d, 4H, tolyl), 6.29 (d, 2H, $H^{1/3}$), 5.20 (t, 1H, H^2), 2.31 (s, 6H, Me). ^{13}C{^{1}H} NMR ($NCCD_3$, 75 MHz, room temperature, δ in ppm): 257.53, CO; 148.29, CH; 142.19, Ph (C^1); 130.64, Ph (C^4); 129.00, Ph ($C^{3/5}$); 128.39; 126.27; 123.88; 123.66; 118.31, Ph ($C^{2/6}$); 89.71; 19.28, Me.

Preparation of IndMo{κ^2-S$_2$CNEt$_2$}(CO)$_2$ (12). A solution of IndMo(η^3-C_3H_5)$(CO)_2$ (0.20 g, 0.65 mmol) in CH_2Cl_2 (15 mL) was treated with HBF_4·Et_2O (1 equiv). After 10 min excess $NEt_2CS_2NH_4$ (0.11 g, 0.75 mmol) was added and the reaction continued for 1 h, after which time the reaction mixture was filtered and the resulting solution taken to dryness. The oily residue was extracted with toluene to give an oil which was extracted with a small portion of ether. By slow concentration and cooling of the Et_2O/hexane (1/5) solution the ruby red crystalline complex was isolated in 70% yield. Anal. Found: C, 46.61; H, 4.10; N, 3.08. Calcd for $C_{16}H_{17}NO_2S_2Mo$: C, 46.27; H, 4.12; N, 3.37. Selected IR (KBr, cm^{-1}): 1940, 1854, vs, ν(CO). ^{1}H NMR ($NCCD_3$, 300 MHz, −40 °C, δ in ppm): 7.24 (s, 4H, H^{5-8}), 6.11 (d, 2H, $H^{1/3}$), 5.29 (t, 1H, H^2), 3.73−3.46 (m, 2H, CH_2), 3.48−3.41 (m, 2H, CH_2), 1.12 (t, 6H, Me).

Preparation of IndMo{κ^2-S$_2$P(OEt)$_2$}(CO)$_2$ (13). A solution of IndMo(η^3-C_3H_5)$(CO)_2$ (0.20 g, 0.65 mmol) in CH_2Cl_2 (15 mL) was treated with HBF_4·Et_2O (1 equiv). After 10 min excess $(OEt)_2PS_2NH_4$ (0.15 g, 0.75 mmol) was added and the reaction continued for 10 h, after which time the mixture was filtered and the resulting solution taken to dryness. The oily residue was extracted with hexane to give the purple crystalline complex in 98% yield. Anal. Found: C, 39.72; H, 4.16. Calcd for $C_{15}H_{17}O_4PS_2Mo$: C, 39.83; H, 3.79. Selected IR (KBr, cm^{-1}): 1956, 1879, vs, ν(CO); 1007. ^{1}H NMR ($NCCD_3$, 300 MHz, −40 °C, δ in ppm): 7.32−7.26 (m, 4H, H^{5-8}), 6.16 (d,

2H, $H^{1/3}$), 5.18 (t, 1H, H^2), 3.62−3.48 (m, 4H, CH_2), 1.15 (t, 6H, Me). $^{13}C\{^1H\}$ NMR ($NCCD_3$, 75 MHz, room temperature, δ in ppm): 254.88, CO; 128.75, $C^{5/8}$; 127.59, $C^{6/7}$; 122.59, $C^{4/9}$; 88.76, C^2; 78.86, $C^{1/3}$; 77.20; 64.99 (CH_2); 16.34 (Me).

Preparation of IndMo(κ^2-acac)$(CO)_2$ (14). A solution of IndMo(η^3-C_3H_5)$(CO)_2$ (0.18 g, 0.58 mmol) in CH_2Cl_2 (15 mL) was treated with HBF_4·Et_2O (1 equiv). After 10 min, excess acetylacetone was added (0.5 mL) and the reaction continued for 2 h. Excess NEt_3 was added, and the mixture was left for 1 h. After that the solution was taken to dryness and the residue was extracted with toluene. The resulting solution was taken to dryness and this powder was recrystallized overnight from Et_2O/hexane at −30 °C. Yield: 88%. Anal. Found: C, 52.39; H, 3.80. Calcd for $C_{16}H_{14}O_4Mo$: C, 52.48; H, 3.85. Selected IR (KBr, cm^{-1}): 1948, 1840, vs, ν(CO). ^1H NMR ($CDCl_3$, 300 MHz, room temperature, δ in ppm): 7.33−7.30 (m, 2H, H^{5-8}), 7.09−7.04 (m, 2H, H^{5-8}), 6.05 (d, 2H, $H^{1/3}$), 5.03 (t, 1H, H^2), 4.75 (s, 1H, −CH), 1.71 (s, 6H, Me). ^1H NMR ($NCCD_3$, 300 MHz, −45 °C, δ in ppm): 7.11 (t, 1H, H^2), 6.41 (s (br), 4H, H^{5-8}), 5.32 (s, 1H, −CH), 4.95 (s (br), $H^{1/3}$), 4.84 (s (br), $H^{1/3}$), 2.31 (s, 3H, Me), 1.89 (s, 6H, Me).

Preparation of IndMo{κ^2-MeCOCHC(NPh)Me}$(CO)_2$ (15). A solution of IndMo(η^3-C_3H_5)$(CO)_2$ (0.20 g, 0.65 mmol) in CH_2Cl_2 (15 mL) was treated with HBF_4·Et_2O (1 equiv). After 10 min $^nBu_4NI$ (0.25 g, 0.70 mmol) was added and the reaction continued for 1 h. The complex $[IndMo(CO)_2I]_2$ was isolated as described in the literature[7f] and dissolved in THF (20 mL). A slight excess of Li{MeCOCHC(NPh)Me} (0.13 g, 0.70 mmol) was added and the reaction continued for 12 h at room temperature, after which time the mixture was taken to dryness. The oily residue thus obtained was washed with small portions of cold toluene and ether to give a pink-red powder. Yield: 65%. Anal. Found: C, 59.82; H, 4.71; N, 3.41. Calcd for $C_{22}H_{19}NO_3Mo$: C, 59.87; H, 4.34; N, 3.17. Selected IR (KBr, cm^{-1}): 1925, 1827, vs, ν(CO).^1H NMR ($NCCD_3$, 300 MHz, room temperature, δ in ppm): 7.60−7.53 (m, 2H, H^{5-8}), 7.48−7.44 (m, 5H, Ph), 7.31−7.27 (m, 2H, H^{5-8}), 6.16 (d, 2H, $H^{1/3}$), 5.58 (t, 1H, CH), 5.06 (t, 1H, H^2), 1.96 (s, 3H, Me), 1.91 (s, 3H, Me).^1H NMR ($NCCD_3$, 300 MHz, −30 °C, after 1 h, δ in ppm): Complex **15** and (η^3-Ind)Mo{η^2-MeC(O)CHC(NPh)-Me}(NCMe)$(CO)_2$, 7.20 (t, 1H, H^2), 6.45−6.42 (m, 2H, H^{5-8}), 6.35−6.33 (m, 2H, H^{5-8}), 5.77 (t, 1H, CH), 4.87 (d, 2H, $H^{1/3}$), 2.06 (s, 3H, coordinated NCMe), 1.96 (s, 3H, CH_3), 1.91 (s, 3H, Me).

Preparation of [(η^3-Ind)Mo(κ^3-ttcn)$(CO)_2$]BF_4 (16). A slight excess of 1,4,7-trithiacyclononane (0.25 g, 1.40 mmol) was added to a solution of $[IndMo(NCMe)_2(CO)_2]BF_4$ (0.28 g, 0.65 mmol) in CH_2Cl_2 (20 mL). The reaction was continued for 2 h at room temperature, after which time the solution was concentrated to ca. 5 mL and ether added to precipitate a light yellow powder. This was further recrystallized from CH_2Cl_2/Et_2O to give the pure compound in 90% yield. Anal. Found: C, 38.03; H, 4.10. Calcd for $C_{17}H_{19}BF_4O_2S_3Mo$: C, 38.22; H, 3.58. Selected IR (KBr, cm^{-1}): 1966, 1892, vs, ν(CO). ^1H NMR (CD_2Cl_2, 300 MHz, −30 °C, δ in ppm): 7.23 (t, 1H, H^2), 6.50−6.46 (m, 2H, H^{5-8}), 6.45−6.40 (m, 2H, H^{5-8}), 4.64 (d, 2H, $H^{1/3}$), 3.04−3.00 (m, 4H, CH_2), 2.91−2.68 (m, 8H, CH_2).

Preparation of (η^3-Ind)Mo(κ^2-$OOCCF_3$)(NCMe)$(CO)_2$ (22). By recrystallization of IndMo(η^2-$OOCCF_3$)$(CO)_2$ from NCMe/Et_2O, dark red crystals of IndMo(η^3-$OOCCF_3$)(NCMe)-$(CO)_2$ are obtained in 98% yield. Anal. Found: C, 42.97; H, 2.24; N, 3.44. Calcd for $C_{15}H_{10}F_3O_4NMo$: C, 42.78; H, 2.39 N, 3.33. Selected IR (KBr, cm^{-1}): 2315, 2288, ν(NC); 1962, 1984, vs, ν(CO); 1692, ν(C═O). ^1H NMR ($NCCD_3$, 300 MHz, −45 °C, δ in ppm): 7.28 (t (br), H^2), 6.46 (m (br), H^{5-8}), 5.19 (s (br), $H^{1/3}$), 4.76 (s (br), $H^{1/3}$).

X-ray Crystallography. Suitable single crystals for the X-ray diffraction studies were grown by standard techniques from saturated solutions of CH_2Cl_2/Et_2O at room temperature. The structure was solved by a combination of direct methods, difference Fourier syntheses, and least-squares methods.

Table 2. Crystallographic Data for [(η^5-Ind)Mo$(CNMe)_2(CO)_2$]BF_4 (2a)

chem formula	$C_{15}H_{13}BF_4MoN_2O_2$
fw	436.02
color/shape	yellow/needle
cryst size (mm)	0.46 × 0.15 × 0.08
cryst syst	monoclinic
space group	$P2_1/c$
a (pm)	725.01(3)
b (pm)	1398.34(9)
c (pm)	1693.49(11)
α (deg)	90
β (deg)	90.990(6)
γ (deg)	90
V (10^6 pm^3)	1716.6(2)
Z	4
T (K)	193
ρ_{calcd} (g cm^{-3})	1.687
μ (cm^{-1})	8.1
F_{000}	864
λ (pm)	71.073
scan method	imaging plate
θ range (deg)	3.17−25.67
data collcd (h,k,l)	±8, ±15, ±20
abs cor	none
transmissn coeff	
no. of rflns collcd	17 303
no. of indep rflns	2179
no. of obsd rflns	2179 (all data)
no. of params refined	254
R_{int}	0.060
R1[a]	0.0697
wR2[b]	0.1650
GOF[c]	1.197
$\Delta\rho_{max/min}$ (e $Å^{-3}$)	+0.56, −0.48

[a] $R1 = \Sigma(||F_o| - |F_c||)/\Sigma|F_o|$. [b] $wR2 = [\Sigma w(F_o^2 - F_c^2)^2/\Sigma w(F_o^2)^2]^{1/2}$. [c] $GOF = [\Sigma w(F_o^2 - F_c^2)^2/(NO - NV)]^{1/2}$; w = SHELXL-93 weights.

Neutral atom scattering factors for all atoms and anomalous dispersion corrections for the non-hydrogen atoms were taken from ref 34. All calculations were performed on a DEC 3000 AXP workstation with the STRUX-V[35] system, including the programs PLATON-92,[36] PLUTON-92,[36] SIR-92,[37] and SHELXL-93.[38]

Data Collection, Structure Solution, and Refinement for Complex 2a. A summary of the crystal and experimental data is reported in Table 2. Preliminary examination and data collection were carried out on an imaging plate diffraction system (IPDS; Stoe & Cie) equipped with a rotating anode (Nonius FR591; 50 kV; 80 mA; 4.0 kW) and graphite-monochromated Mo Kα radiation. Data collection was performed at 193 (293) K within the θ range of $2.2° < \theta < 25.7°$ with an exposure time of 3.0 min per image (oscillation scan modus from $\varphi = 0.0°$ to 360° (230°) with $\Delta\varphi = 1°$). A total number of 17 303 (12 913) reflections were collected; 941 (789) negative and systematic absent 189 (122) reflections were rejected from the original data set. After merging, a total of 2179 (2984) independent reflections remained and were used for all calculations. Data were corrected for Lorentz and polarization effects. All crystals of compound **2a** were found to be twinned.

(34) *International Tables for Crystallography*; Wilson, A. J. C., Ed.; Kluwer Academic Publishers: Dordrecht, The Netherlands, 1992; Vol. C, Tables 6.1.1.4 (pp 500−502), 4.2.6.8 (pp 219−222), and 4.2.4.2 (pp 193−199).

(35) Artus, G.; Scherer, W.; Priermeier, T.; Herdtweck, E. STRUX-V, a Program System To Handle X-ray Data; TU München: München, Germany, 1997.

(36) Spek, A. L. PLATON-92-PLUTON-92, An Integrated Tool for the Analysis of the Results of a Single-Crystal Structure Determination. *Acta Crystallogr., Sect. A* **1990**, *46*, C34.

(37) Altomare, A.; Cascarano, G.; Giacovazzo, C.; Guagliardi, A.; Burla, M. C.; Polidori, G.; Camalli, M. SIR-92; University of Bari: Bari, Italy, 1992.

(38) Sheldrick, G. M. SHELXL-93 In *Crystallographic Computing 3*; Sheldrick, G. M., Krüger, C., Goddard, R., Eds.; Oxford University Press: London, 1993; pp 175−189.

Therefore, raw data were reduced with the program *Twin*.[39] The unit cell parameters were obtained by full-matrix least-squares refinements of 4354 (1804) reflections with the program Cell.[39] All "heavy atoms" of the asymmetric unit were anisotropically refined. Hydrogen atoms were calculated in ideal positions (riding model), included in the structure factor calculations, but not refined. Full-matrix least-squares refinements were carried out by minimizing $\Sigma w(F_o^2 - F_c^2)^2$ with the SHELXL weighting scheme and stopped at shift/error < 0.001.

Molecular Orbital Calculations

Extended Hückel Calculations. EH calculations were performed using the ICON8 program[22a,b] with modified H_{ij} values.[22c] The basis set for the metal atoms consisted of *n*s, *n*p, and (*n* − 1)d orbitals. The s and p orbitals were described by single Slater-type wave functions, and the d orbitals were taken as contracted linear combinations of two Slater-type wave functions. Only s and p orbitals were considered for P. The parameters used for Mo were as follows (H_{ii} (eV), ζ): 5s −8.77, 1.960; 5p −5.60, 1.900; 4d −11.06, 4.542 (ζ_1), 1.901 (ζ_2), 0.5899 (C_1), 0.5899 (C_2). Standard parameters were used for other atoms. Three-dimensional representations of orbitals were drawn using the program CACAO.[40]

The calculations were performed on model complexes with idealized geometries and C_s symmetry, taken from the real structures quoted along the text. Thus, $[(\eta^3\text{-Ind})MoL_2(CNMe)(CO)_2]^+$ (L = NCMe, CNMe, PH_3) complexes were taken as perfect octahedrons, with all L-Mo-L angles equal to 90°; the η^3 coordination mode of the indenyl ligand was accomplished by bending the ring across C1−C3 by 30° (see Chart 1). $[(\eta^5\text{-Ind})MoL_2(CO)_2]^+$ species have a piano-stool geometry with Ind−Mo−X angles of 115°. This value, as well as the rotational conformation of the indenyl ligand in all the models, was the result of a geometry optimization. The bond distances (Å) were as follows: M−(C5 ring centroid), 2.00; M−C(CO), 2.00; Mo−N, 2.17; Mo−C(CNMe), 2.17; Mo−P, 2.47; C−O, 1.15; C−N, 1.13; C−C (NCMe), 1.45; C−C, 1.40; C−H, 1.08; P−H, 1.4.

DFT Calculations. Density functional calculations[23] were carried out on model compounds based on the structures of **2a** for the $[(\eta^5\text{-Ind})MoL_2(CO)_2]^+$ complexes and that of $[(\eta^3\text{-Ind})Mo(NCMe)_2(CO)_2]^+$,[18] under C_s symmetry, using the Amsterdam Density Functional (ADF) program[24] developed by Baerends and co-workers.[41] The slipping, folding, and position of the indenyl and the bending of the equatorial ligands were optimized. Vosko, Wilk, and Nusair's local exchange correlation potential was used,[42] with Becke's nonlocal exchange[43] and Perdew's correlation corrections.[44] The geometry optimization procedure was based on the method developed by Versluis and Ziegler,[45] using the nonlocal correction terms in the calculation of the gradients. The core orbitals were frozen for Mo ([1−3]s, [1−3]p, 3d) and C, N, and O (1s). Triple-ζ Slater-type orbitals (STO) were used for H 1s, C, N, and O 2s and 2p, and Mo 4s and 4p. A set of polarization functions was added: H (single ζ, 2p); C, N, and O (single ζ, 3d).

Acknowledgment. This work was supported by PRAXIS XXI under projects 2/2.1/QUI/316/94 and PBIC/C/QUI/2201/95. I.S.G. (BPD) and C.A.G. (BD) thank PRAXIS XXI for grants.

Supporting Information Available: Tables of data collection parameters, bond lengths, bond angles, fractional atomic coordinates, and thermal parameters (6 pages). Ordering information is given on any current masthead page.

OM971005G

(39) IPDS Operating System, Version 2.8; Stoe & Cie GmbH, Darmstadt, Germany, 1997.

(40) Mealli, C.; Proserpio, D. M. *J. Chem. Educ.* **1990**, *67*, 39.

(41) (a) Baerends, E. J.; Ellis, D.; Ros, P. *Chem. Phys.* **1973**, *2*, 41. (b) Baerends, E. J.; Ros, P. *Int. J. Quantum Chem.* **1978**, *S12*, 169. (c) Boerrigter, P. M., te Velde, G.; Baerends, E. J. *Int. J. Quantum Chem.* **1988**, *33*, 87. (d) te Velde, G.; Baerends, E. J. *J. Comput. Phys.* **1992**, *99*, 84.

(42) Vosko, S. H.; Wilk, L.; Nusair, M. *Can. J. Phys.* **1980**, *58*, 1200.

(43) Becke, A. D. *J. Chem. Phys.* **1987**, *88*, 1053.

(44) (a) Perdew, J. P. *Phys. Rev.* **1986**, *B33*, 8822. (b) Perdew, J. P. *Phys. Rev.* **1986**, *B34*, 7406.

(45) (a) Versluis, L.; Ziegler, T. *J. Chem. Phys.* **1988**, *88*, 322. (b) Fan, L.; Ziegler, T. *J. Chem. Phys.* **1991**, *95*, 7401.